European Journal of Taxonomy 826: 135–162
https://doi.org/10.5852/ejt.2022.826.1841
ISSN 2118-9773
www.europeanjournaloftaxonomy.eu
2022 · Hoffman L. *et al.*

Research article

urn:lsid:zoobank.org:pub:09635D60-D052-4C7A-B4B7-1F1962D08051

Abyssal vent field habitats along plate margins in the Central Indian Ocean yield new species in the genus *Anatoma* (Vetigastropoda: Anatomidae)

Leon HOFFMAN[1,*], Katharina KNIESZ[2], Pedro MARTÍNEZ ARBIZU[3] & Terue C. KIHARA[4]

[1,2,3] Senckenberg am Meer, Südstrand 40-44, Wilhelmshaven, 26382, Germany.
[2,3] Carl von Ossietzky Universität Oldenburg, Oldenburg, Germany.
[4] INES Integrated Environmental Solutions UG, Südstrand 40-44, 26382, Wilhelmshaven, Germany.

[*] Corresponding author: Leon.Hoffman@Senckenberg.de
[2] Email: Katharina.Kniesz@Senckenberg.de
[3] Email: Pedro.Martinez@Senckenberg.de
[4] Email: Terue.Kihara@ines-solutions.eu

[1] urn:lsid:zoobank.org:author:55E2A441-915A-4EB0-B3DC-4A2CD03B1844
[2] urn:lsid:zoobank.org:author:C32DD126-EC38-4D82-B688-99E70C24018D
[3] urn:lsid:zoobank.org:author:FC6F29CE-477E-476F-911F-D1BF5125C514
[4] urn:lsid:zoobank.org:author:CFD7345A-AFE1-4848-8D96-37C49B163FFA

Abstract. New species in *Anatoma* Woodward, 1859 (Anatomidae, Vetigastropoda) are found in abyssal hydrothermal vent field habitats on the oceanic plate margins in the Indian Ocean. Six species are identified using molecular sequence analyses of which four species are described as new based on their morphological characters: *Anatoma discapex* sp. nov., *Anatoma declivis* sp. nov., *Anatoma laevapex* sp. nov. and *Anatoma paucisculpta* sp. nov. Inadequate material was available for a morphological description of the other two species with genetic identification, but it is likely that all six species are new to science and endemic to the Indian Ocean. The northern Central Indian Ridge localities are dominated by *Anatoma declivis* sp. nov.; its closest relative is *Anatoma discapex* sp. nov. which occurs in the central area near the Rodriguez Triple Junction. *Anatoma laevapex* sp. nov. and *Anatoma paucisculpta* sp. nov. as well as a fifth undescribed species are mainly found on the Southeast Indian Ridge.

Keywords. Indian Ocean, hydrothermal vents, *Anatoma*, Gastropoda, INDEX project.

Hoffman L., Kniesz K., Martínez Arbizu P. & Kihara T.C. 2022. Abyssal vent field habitats along plate margins in the Central Indian Ocean yield new species in the genus *Anatoma* (Vetigastropoda: Anatomidae). *European Journal of Taxonomy* 826: 135–162. https://doi.org/10.5852/ejt.2022.826.1841

Introduction

As a part of the research executed by the German Federal Institute for Geosciences and Natural Resources (BGR) to identify inactive polymetallic sulphide deposits along the Central Indian Ridge (CIR) and the

Southeast Indian Ridge (SEIR), the INDEX project conducted cruises to the oceanic plate margins in the Indian Ocean in 2015, 2018 and 2019 with the aim to investigate geological, geophysical and biological aspects of hydrothermal vent developments. These vents include morphological structures from outflow of hydrothermal water and gases that are commonly found at diverging oceanic plate margins. The structures are often referred to as black or white smokers. Significant variations of chemical compositions in seawater and on the seafloor, as well as wide hydrothermal variations, yield a large number of microhabitats for marine life.

Knowledge of the hydrothermal vent fauna is an important tool to detect vulnerable taxa and can be used to designate marine protected areas. The investigation of biodiversity at these sites is an objective of activity related to the INDEX project, with recent studies mapping the vent fauna and describing benthic assemblages along the German claim showing that Mollusca account for a considerable number of benthic taxa (Gerdes *et al*. 2019a, 2019b, 2021). Similar observations were reported from other vents of the Central Indian Ridge (CIR) (Hashimoto *et al*. 2001; Van Dover *et al*. 2001; Van Dover 2002; Nakamura *et al*. 2012; Watanabe & Beedessee 2015; Kim *et al*. 2020) and Southwest Indian Ridge (SWIR) (Zhou *et al*. 2018; Sun *et al*. 2020).

From the known species, gastropods representing the families Cancellariidae (*Iphinopsis boucheti* Okutani, Hashimoto & Sasaki, 2004), Skeneidae (*Bruceiella wareni* Okutani, Hashimoto & Sasaki, 2004) and Provannidae (*Desbruyeresia marisindica* Okutani, Hashimoto & Sasaki, 2004, *Alviniconcha marisindica* Okutani, 2014) were described over the past decades (Okutani *et al*. 2004; Johnson *et al*. 2015).

Special attention was paid to the family Peltospiridae (Chen *et al*. 2015a, 2015b, 2017, 2021), with the description of the iconic scaly-foot snail *Chrysomallon squamiferum* C. Chen, Linse, Copley & Rogers, 2015, *Gigantopelta aegis* C. Chen, Linse, Roterman, Copley & Rogers, 2015, *Dracogyra subfusca* C. Chen, Y.-D. Zhou, C.-S. Wang & Copley, 2017, *Lirapex politus* C. Chen, Y.-D. Zhou, C.-S. Wang & Copley, 2017 and *Lirapex felix* C. Chen, Y.-R. Han, Copley & Y.-D. Zhou, 2021.

Anatomidae McLean, 1989 live on a large variety of sea bottoms, from intertidal zones to abyssal depths in all oceans of the world. The dominant genus with 82 known species is *Anatoma* Woodward, 1859, which contains about 98.8% of species in Anatomidae; one species is in the genus *Sasakiconcha* Geiger, 2006 (WoRMS 2020). Geiger (2012) completed the first global revision of "little slit shells" that included the family Anatomidae. He described and imaged all hitherto known species in great detail and a large part of the knowledge regarding this genus is comprised in his monograph. Geiger (2012) reported 14 species from the Indian Ocean, but only two of them have been reported living in abyssal depths exceeding 2000 m (Table 1). To our knowledge, no results from studies on species in *Anatoma* from vent habitats in the Indian Ocean have been published to date.

The present paper contributes to the study of the biodiversity in vent habitats discussing molecular species delimitation and the possibility that small vetigastropods can develop a high degree of endemism along oceanic plate margins. Using integrated taxonomy, it also provides descriptions of four new species of the genus *Anatoma* Woodward, 1859 (Anatomidae), as well as their abundances and distributions on the CIR and SEIR.

Material and methods

Area of investigation

This study focusses on locations in vent fields found within the licence blocks held by the German Federal Institute for Geosciences and Natural Resources (BGR) on the Central Indian Ridge (CIR) and Southeast Indian Ridge (SEIR) in the central Indian Ocean (Fig. 1).

Table 1. Anatomidae McLean, 1989 from the Indian Ocean as given by Geiger (2012). The last four species are described as new in this study.

Species	Depth range (m)	Distribution
Anatoma africanae (Barnard, 1963)	400	SW Indian Ocean, Gallieni Fracture Zone
Anatoma agulhasensis (Thiele, 1925)	49–500	Shelf E Africa
Anatoma austrolissa Geiger & Sasaki, 2008	640–1600	SW Pacific, Réunion
Anatoma biconica Geiger, 2012	475–932	SW Pacific, SE Africa, Madagascar
Anatoma boucheti Geiger & Sasaki, 2008	1150–1180	Réunion
Anatoma finlayi (Powell, 1937)	92–903	SW Pacific, Madagascar, Réunion
Anatoma flexidentata Geiger & Sasaki, 2008	280–1620	SW Pacific, Mozambique, Réunion
Anatoma japonica (A. Adams, 1862)	6–1000	W Pacific, W Indian Ocean (incl. Réunion, Madagascar)
Anatoma munieri (Fischer, 1862)	15–2650	W Pacific, W Australia, Oman
Anatoma planapex Geiger, 2012	150–1371	Australia, Solomon Islands
Anatoma porcellana Geiger, 2012	49–2570	W Pacific, Madagascar
Anatoma tabulata (Barnard, 1964)	184–805	SE Africa, Madagascar
Anatoma yaroni Herbert, 1986	295–1200	SW Indian Ocean (incl. Réunion, Madagascar)
Anatoma discapex sp. nov.	2560–3296	CIR
Anatoma declivis sp. nov.	2469–3082	CIR, SEIR
Anatoma laevapex sp. nov.	2469–3048	CIR, SEIR
Anatoma pauciculpta sp. nov.	2480–3296	CIR, SEIR

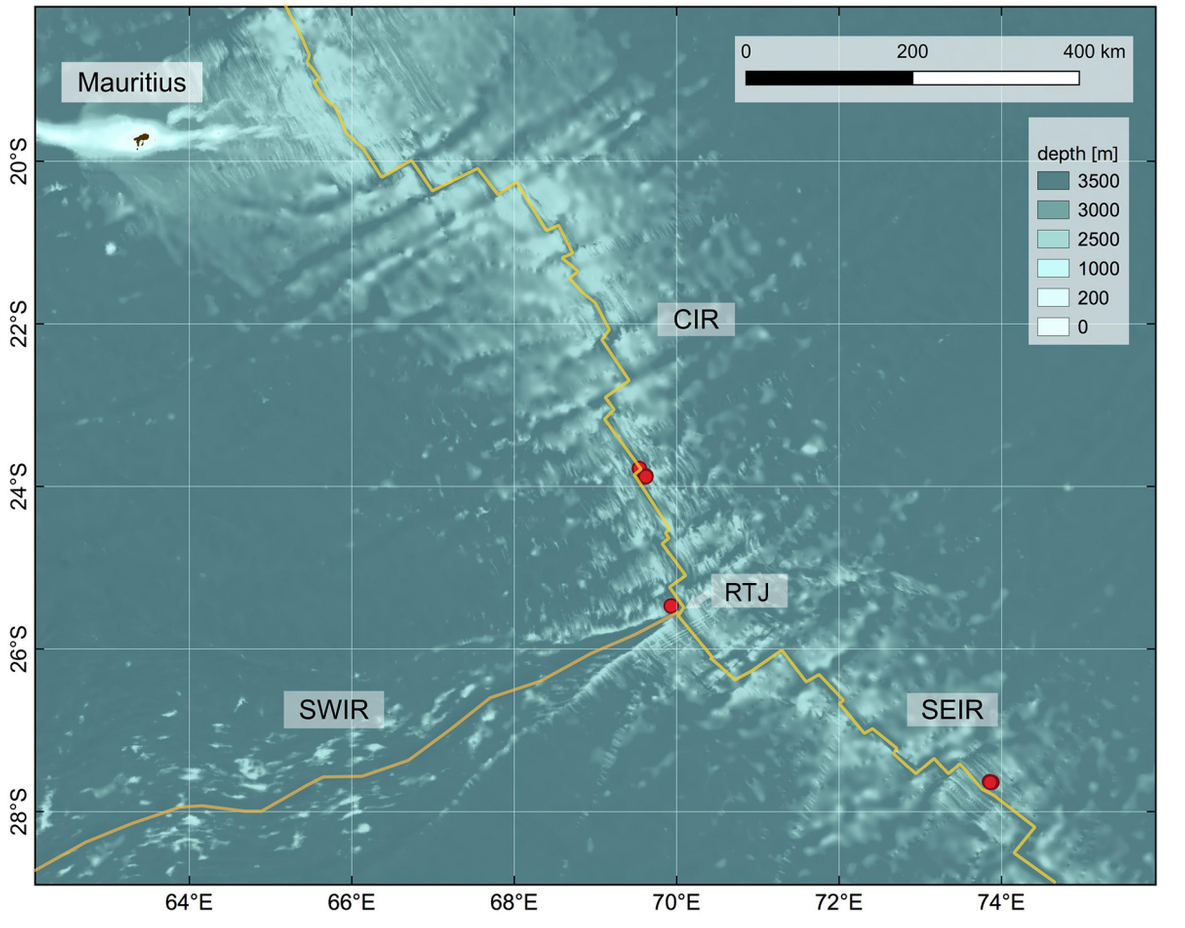

Fig. 1. Location map of oceanic plate ridges in the central Indian Ocean. Three areas are indicated by red dots where species in *Anatoma* Woodward, 1859 were encountered. Abbreviations: CIR = Central Indian Ridge; RTJ = Rodriguez Triple Junction; SEIR = SE Indian Ridge; SWIR = SW Indian Ridge. Map by QGIS using GEBCO bathymetry data.

Sampling methods

The material used for the study of *Anatoma* was collected during the INDEX2015, INDEX2018 and INDEX2019 cruises on the research vessels *Pelagia* and *Sonne* using the Canadian ROV (Remotely Operated Vehicle) ROPOS (Remotely Operated Platform for Ocean Sciences). All samples have been taken by ROV-operated manipulators (grabs and suction device) and sampling information is listed in Table S1 (Supp. file 1). Live species have often been sampled as associated fauna with sediment and rock samples. Biological specimens have been collected by hand pickings and they have been sorted at species level and stored in ethanol (96%). Part of the samples has been kept under cooled or frozen condition to enable reliable genetic analyses at DZMB in Wilhelmshaven.

From the material obtained during three cruises from six different vent field areas, each specimen received a unique reference number (voucher specimen code). Detailed specimen data (taxonomy, collection sites, voucher specimen codes and museum number) is available in Barcode of Life Data Systems (BOLD; www.boldsystems.org) (Ratnasingham & Hebert 2007), project "Indian Ocean Hydrothermal Vent Fauna – INDEX" – subproject "Indian Ocean Hydrothermal Vent Macrofauna" in the public dataset "DS-INMAC03".

Imaging

To enable specific determination, each specimen used for former molecular analyses has been photographed with a Leica MZ 95 binocular microscope and a Lumix DMC – TZ 5 camera. This image set has been used to complete a species classification. Specimens within each species have subsequently been selected for morphological imaging of the soft parts and for the shells. Imaging of the soft parts has been carried out after removal of the shell by organic acid; the imaging has been done using a confocal laser scanning microscope (CLSM) at DZMB. Imaging of the shells has been done using a VEGA3-Tescan scanning electron microscope (SEM). Species descriptions are based on the photo sets for each species.

Molecular methods

After the morphological identification, several specimens of *Anatoma* were processed molecularly (Supp. file 1: Table S1). For 169 specimens genomic DNA (Supp. file 1: Table S1) was extracted by removing the soft part of the gastropod from the shell by microwaving for some seconds in a glass vial filled with water (Galindo *et al.* 2014). Further, 30 µl of CHELEX (BIO-RAD Insta Gene Matrix) was added and heated for 20 minutes at 56°C and 10 minutes at 99°C. For some samples the extraction was performed using columns to receive higher concentrated DNA (E.Z.N.A.® Mollusc DNA Kit, NucleoSpin® Tissue) following the manufacturer's protocol.

For the PCR, the primer pair jgHCO2198/jgLCO1490 (Geller *et al*. 2013) with M13 tails was used to define nucleotide sequences for sequencing. For PCR, AccuStart II PCR SuperMix with a total volume of 12.5 µl (6.25 µl of AccuStart, 4.75 µl of H20, 0.25 µl of each primer and 1 µl of DNA) was added. Specimen that failed with the long fragment of COI were redone with the primer pair Lobo F1 and Lobo R1 (Lobo Arteaga *et al*. 2013) in combination with the abovementioned named primer pair and the same protocol. These primers resulted in shorter fragments and are appropriate for defragmented DNA. All amplified products were purified using Exo-SAP-IT ®. Finally, the PCR-products were sent to the Macrogen Europe Laboratory in Amsterdam for sequencing.

The obtained sequences of *Anatoma* were cleaned using Geneious Prime® 2020.1.2 (Kearse *et al*. 2012) to check for ambiguities and errors. All edited sequences were aligned and trimmed with MAFFT (Katoh *et al*. 2002) alignment in Geneious. Short sequences and sequences with bad quality were not included in the analysis. Afterwards, similarity analyses were done with BLASTn (Nucleotide BLAST) (Altschul *et al*. 1990) search against GenBank and BOLD (Ratnasingham & Hebert 2007).

Table 2. List of COI sequences from GenBank for the genus *Anatoma* Woodward, 1859 used for the molecular analyses in this study. Species name, GenBank accession number, locality, habitat and reference are given.

Species name	GenBank accession no.	Locality	Habitat	Reference
Anatoma euglypta (Pelseneer, 1903)	AY923934	Antarctica	–	Geiger & Thacker 2005
Anatoma pseudoequatoria (Kay, 1979)	MW278816	Hawai	reef and shore	unpublished
Anatoma sp. Izu	AB365211	Izu, Shizuoka, Japan	intertidal	Kano 2008
Anatoma sp. Lau	AB365210	Lau Basin	hydrothermal vents	Kano 2008

Species delimitation and phylogenetic analyses

Combining our dataset of 95 sequences of COI with the four available sequences for *Anatoma* from GenBank (Table 2) we try to infer the number of sampled species and their classification or relation within the genus *Anatoma*. Therefore, the genetic distances of Molecular Taxonomical Units (MOTUs) were analysed. These MOTUs were ascertained with five methods using the COI dataset consisting of 95 sequences.

First of all, intra- and interspecific distances for our dataset were calculated by the Barcode Gap Analysis provided by BOLD. As a result, the threshold value that is mandatory for some delimitation methods was set at 0.983 or 98.3% (mean intraspecific divergence is 1.7%) (Supp. file 1: Fig. S1, Table S2).

The used delimitation methods can be grouped into three distance-based and two tree-based methods. Automatic Barcode Gap Discovery (ABGD) is calculating the "barcoding gap" (threshold distance) between inter- and intraspecific variation (Puillandre *et al*. 2012). Another distance-based method is CD-HIT (Li & Godzik 2006), a heuristic clustering process that requires defined sequence similarity thresholds. The third method of delimitation that uses calculated distances is the Barcode Index Numbers (BINs) system implemented in BOLD (Ratnasingham & Hebert 2013). This system registers each cluster of sequences and assigns a unique and specific code (BIN).

In contrast, the following two methods build groups of species based on a tree. General Mixed Yule Coalescent (GMYC) is a method that determines the point of transition from speciation to coalescent branching patterns (Pons *et al*. 2006; Monaghan *et al*. 2009). Another method is the Bayesian Poisson Tree Process (BPTP) for larger datasets (Zhang *et al*. 2013).

To present the different MOTUs and morphospecies in a graphic way, Bayesian tree analyses were performed. Therefore, the best fitting model was determined by the modeltest using MEGA X (Kumar *et al*. 2018) using both the Akaike Information Criterion (AIC) and the Bayesian Information Criterion (BIC). The best model for our dataset was the Tamura-Nei (TN93+G) model. For the construction of the tree, BEAST ver. 1.8.3 package and Yule-coalescent model as implemented in the R package 'splits' (Suchard *et al*. 2018) were used. The tree was produced and annotated with Bayesian posterior probabilities (PP) using TreeAnnotator in the BEAST ver. 1.8.3 package.

Sample retention

DNA extracts and material with soft parts in ethanol are stored at the DZMB. Type specimens with shells are retained at the Senckenberg Naturmuseum in Frankfurt am Main (SMF), Germany. DNA information has been deposited in the GenBank data base.

All coordinates of locations have been converted to decimal format to facilitate their use in databases and mapping.

Abbreviations

ABGD = Automatic Barcode Gap Discovery
BIN = Barcode Index Number
BOLD = Barcode of Life Data System
bp = base pairs
BPTP = Bayesian Poisson Tree Processes
CIR = Central Indian Ridge
CLSM = Confocal Laser Scanning Microscope
COI = Cytochrome c oxidase subunit I, a protein
DZMB = Deutsches Zentrum für Marine Biodiversitätsforschung
GMYC = Generalized Mixed Yule-Coalescent
H = height of shell
Ha = height of aperture
ISD = Intra-specific Distance
MAFFT = Multiple Alignment using Fast Fourier Transform
MOTU = Molecular Operational Taxonomic Unit
ROV = remotely operated vehicle
RTJ = Rodriguez Triple Junction
SEIR = SE Indian Ridge
SEM = Scanning Electron Microscope
SMF = Senckenberg Naturmuseum, Frankfurt am Main
SWIR = SW Indian Ridge
W = maximum width of shell
Wp = maximum width of protoconch

Results

Molecular analyses

A total of 643 anatomid specimens were collected from the sediment samples during this study. A subset of 95 specimens could be identified as 6 different MOTUs (Fig. 2 and Table 3). Two MOTUs are only represented by a single specimen. In this study, 95 high-quality sequences of COI were obtained (Table 3 and Supp. file 1: Table S1). Fragment lengths ranged from 513 to 658 bp; no indels (genetic insertions or deletions in genomes) or stop codons were found. In addition, a subset of 17 sequences of shorter fragments of COI was analysed (306–339 bp).

The molecular species delimitation methods revealed 5 to 6 MOTUs (Fig. 2). Plausible consensus clusters were maintained by combining all the methods and creating consensus clusters for conforming results of at least three methods. As a result, six MOTUs with four clusters and two singletons (Fig. 2) were identified. The four clusters will be described in the following part. The two singletons remain undescribed (*Anatoma* sp. 1 DZMB_2021_0095, *Anatoma* sp. 2 DZMB_2021_0096).

The maximum intra-specific distances in the COI sequence are less than 1.5% (mutations in ca 10 bp in the investigated COI sequence) for all species whereas the inter-species distances are more than 6% (mutations in ca 40 bp) between all investigated species. The mean intra-specific distance is less than 0.6% for all species.

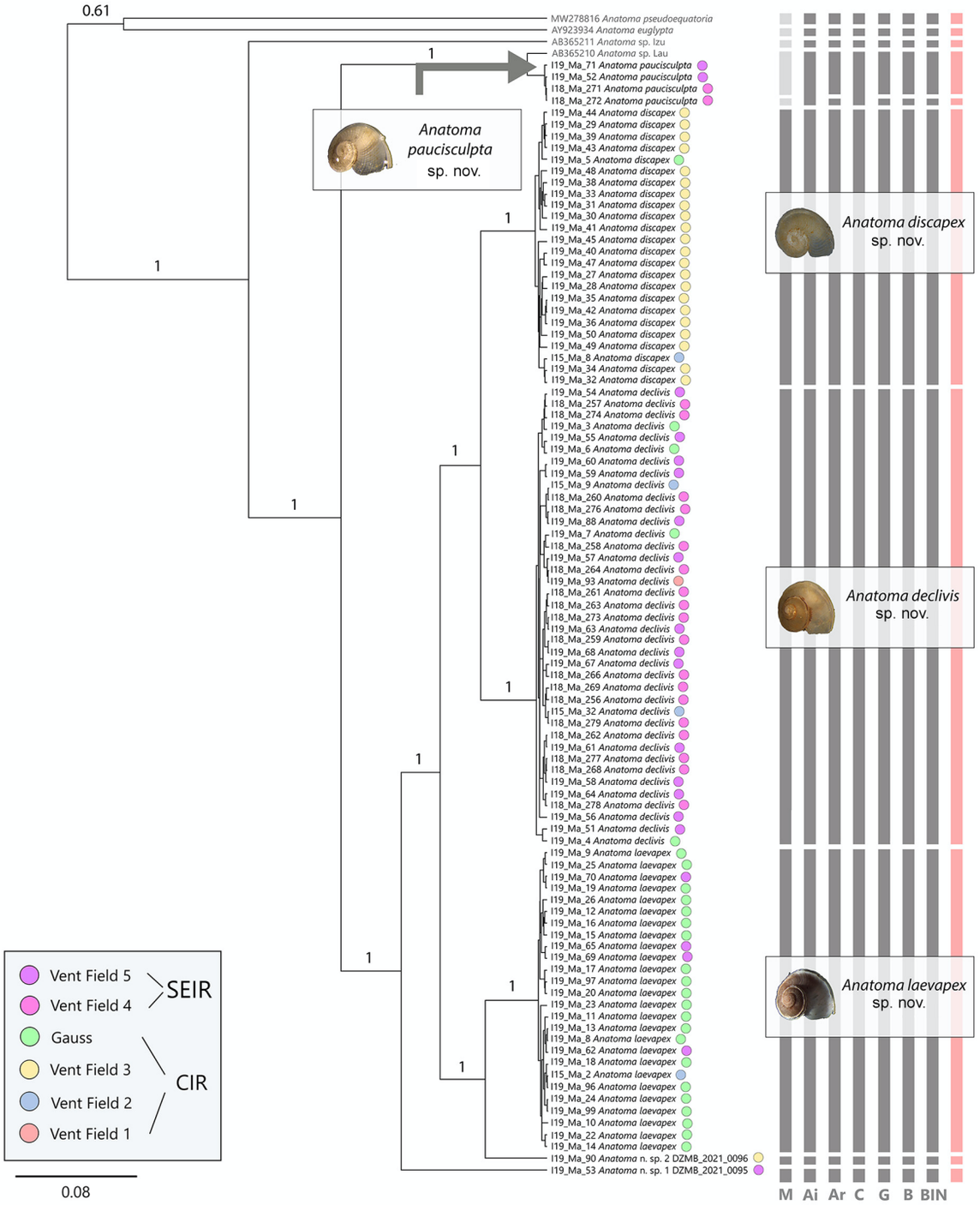

Fig. 2. Bayesian inference tree of 95 individuals based on a MAFFT alignment showing posterior probabilities. Included are four COI sequences from GenBank (marked in grey, Table 2), locations of findings are colour coded. Relevant species delimitation result is shown by six bars: M = morphology; Ai = ABGD (initial partition); Ar = ABGD (recursive partition); C = CD-Hit; G = GMYC; B = BPTP and BIN. The red bar presents the consensus of all delimitation methods.

Table 3. The list of taxa identified in the study presented for the sampled location: Gauss vent field (Gau), Vent field (VF). Unidentified or juvenile specimen are not named (see Supp. file 1: Table S1). Selected sequences for COI, morphological delimitation (M), MOTUs for ABGD (Ai, initial and Ar, recursive partition), CD-Hit (C), GMYC (G) and bPTP (B).

Species	No. of individuals						No. of seq's	Species delimitation methods					
	Gau	VF1	VF2	VF3	VF4	VF5		M	Ai	Ar	C	G	B
Anatoma declivis sp. nov.	5	18	9	7	147	16	39	1	1	1	1	1	1
Anatoma discapex sp. nov.	5	28	5	32	38	–	24	1	1	1	1	1	1
Anatoma laevapex sp. nov.	24	2	1	–	68	8	26	1	1	1	1	1	1
Anatoma pauciculpta sp. nov.	–	1	–	–	6	3	4	1	1	1	1	1	1
Anatoma 1 DZMB_2021_0095	–	–	–	–	–	1	1	1	1	1	1	1	1
Anatoma 2 DZMB_2021_0096	–	–	–	1	–	–	1	1	1	1	1	1	1
Total numbers	34	49	15	40	259	28	95	6	6	6	6	6	6

The comparison with reference libraries (GenBank and BOLD) shows the highest identity to *Anatoma* sp. Lau (Kano 2008) (82–98% identity; GenBank accession number: AB365210). According to species delimitation analysis, all *Anatoma* records from literature (Table 2) are clearly separated from our species, except the species *Anatoma* sp. Lau (Fig. 2). Nevertheless, the consensus indicated this species to be separate from all other anatomid species in this study.

All sequences were deposited in GenBank with the accession numbers: OM951021-OM951133. Relevant voucher information, pictures, taxonomic classifications, and sequences are deposited in the dataset "DS-INMAC03" in the Barcode of Life Data System (BOLD) (www.boldsystems.org) (Ratnasingham & Hebert 2007) (GenBank accession numbers in Supp. file 1: Table S1).

Systematics

Class Gastropoda Cuvier, 1795
Subclass Vetigastropoda Salvini-Plawen, 1980
Superfamily Scissurelloidea Gray, 1847
Family Anatomidae McLean, 1989

Genus ***Anatoma*** Woodward, 1859

Type species

Anatoma crispata (J. Fleming, 1828), type by monotypy.

Anatoma discapex sp. nov.
urn:lsid:zoobank.org:act:8662D87B-3AC7-4F7D-8A34-AA8A64965174
Figs 3–4

Etymology

The species name '*discapex*' refers to the flattened apex.

Type material

Holotype

INDIAN OCEAN • CIR; 25.47° S, 69.93° E; depth 2628 m; 16 Nov. 2019; stn INDEX19_042RO; spec. I19_Ma_84, SEM, Fig. 3A–B; SMF 358976.

Paratypes

INDIAN OCEAN • 1 specimen (paratype 1); same location data as for holotype; SEM, Fig. 3C–D; SMF 358977 • 1 specimen (paratype 2); same location data as for holotype; spec. I19_Ma_85, SEM, Fig. 3E–F; SMF 358978 • 1 specimen (paratype 3); CIR; 23.88° S, 69.62° E; depth 3082 m; 11 Nov. 2019; stn INDEX19_031RO; spec. I19_Ma_86, Fig. 3G–H, SEM; SMF 358979 • 1 specimen (paratype 4); same location data as for preceding; SEM, Fig. 3I–K; SMF 358980 • 1 specimen (paratype 5); same location data as for preceding; spec. I19_Ma_80, SEM, Fig. 3L–N; SMF 358981 • 1 specimen (paratype 6); same location data as for preceding; spec. I19_Ma_81, SEM, Fig. 3O–Q; SMF 358982 • 1 specimen (paratype 7); same location data as for preceding; spec. I19_Ma_79, SEM, Fig. 3R–S; SMF 358983.

Other material examined

INDIAN OCEAN • 1 specimen; CIR; 23.87° S, 69.62° E; depth 3032 m; 12 Nov. 2019; stn INDEX19_033RO; spec. I19_Ma_5 • 24 specimens; 25.47° S, 69.93° E; depth 2628 m; 16 Nov. 2019; stn INDEX19_042RO; specs I19_Ma_27–50 • 5 specimens; 23.78° S, 69.55° E; depth 3049 m; 2 Dec. 2015; stn INDEX15_49R; specs I15_Ma_8, I15_Ma_133, I15_Ma_135–136, I15_Ma_144 • 8 specimens; 23.88° S, 69.62° E; depth 3296 m; 8 Dec. 2015; stn INDEX15_62R; specs I15_Ma_145, I15_Ma_147–150, I15_Ma_154, I15_Ma_158, I15_Ma_163.

Shell description

Protoconch (Fig. 3K of paratype 4). One flat whorl, coarse pitted sculpture; raised flexuous lip with rim at transition to teleoconch, transition clear by change in sculpture; diameter 0.20 mm.

Teleoconch (Fig. 3A–B). Flattened upper spire and disk-shaped outline with strongly protruding margins of selenizone; flexuous axial ribs; pear-shaped aperture with slit; suture deep. Height 1.3 mm, width 2.1 mm, height of aperture 0.85 mm (60 % of total height); colour opaque grayish white. 2¼ regular whorls with flattened, slightly convex shoulder area and rounded base, selenizone slightly above periphery; suture well below selenizone of penultimate whorl in last half of body whorl. Teleoconch I from protoconch to start of selenizone: ¾–1 convex whorl, in plane with protoconch; about 15 strong axial ribs, flexuous; no spiral cord. Teleoconch II with selenizone: initial whorl about 30 axial ribs, last ¼ whorl of body whorl about 22 axial ribs; bifurcating and closely spaced near lip. Margins of selenizone sharply protruding upwards or sideways near the lip. Axial ribs on external margins of selenizone; inside margins smooth. Frequency of axial ribs below selenizone similar to that above; rough growth lines between ribs, typically 3–6 major stages. Umbilicus open, tortuous and deep; steeply spiralling keel at union of columellar callus with parietal area (Fig. 3A of holotype and 3C, E, G of paratypes).

Aperture (Fig. 3A). Rounded base, funnel-shaped towards selenizone, pointed at union with penultimate whorl. Columellar lip sharp, protruding, rounded at base, flexuous towards parietal area; parietal callus thin and reclining. Semi-circular lower lip; slit slightly above periphery with concave edge of lip on either side, slit ¼ whorl deep with flattened sharp margins above and below. Callus thin; inside aperture smooth.

Variation. Little morphological variation of shell. Variable length of selenizone I and number of axial ribs. Adult height range 1.1–1.4 mm; width range 2.1–2.2 mm.

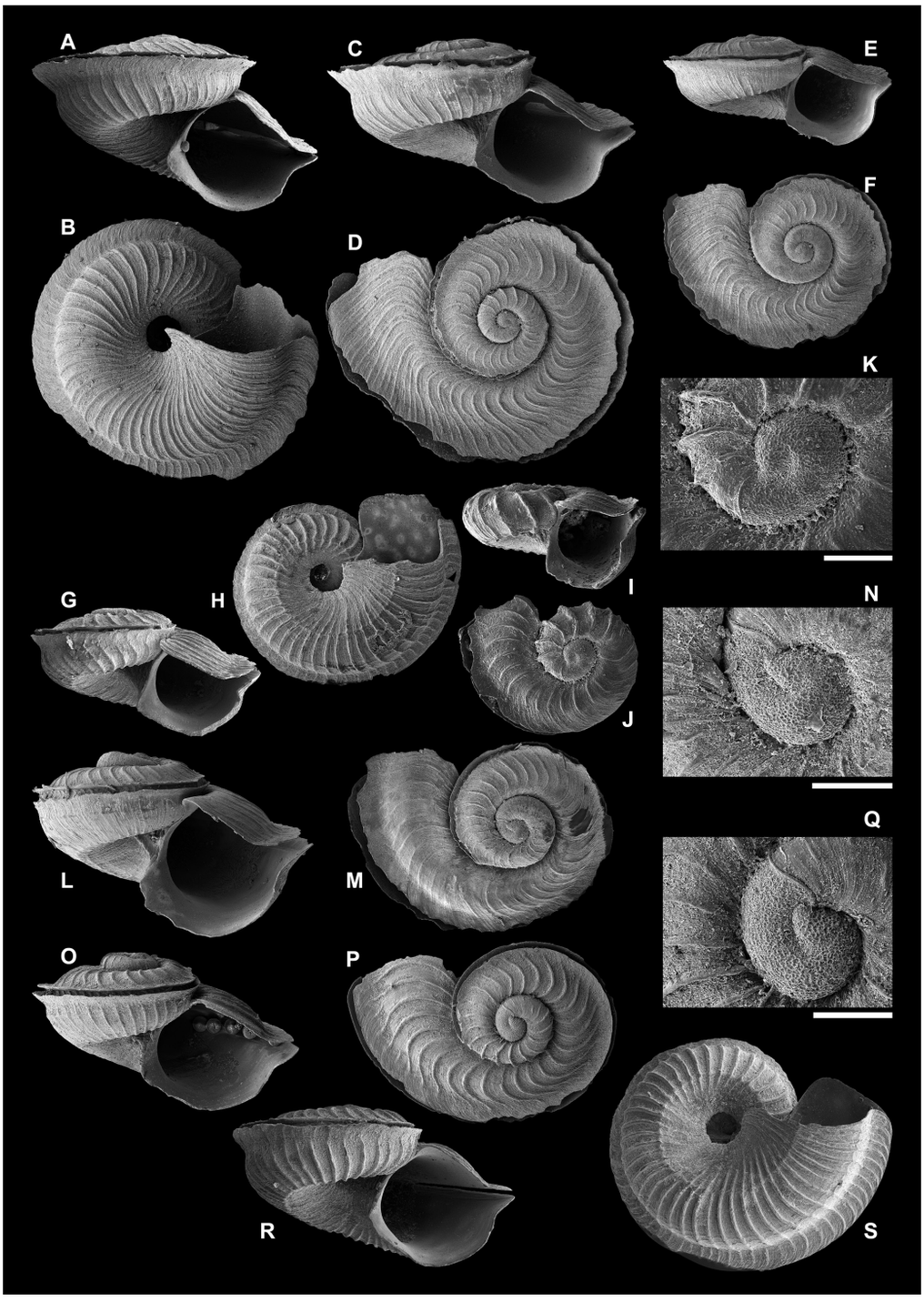

Fig. 3. *Anatoma discapex* sp. nov. **A–F**. INDEX19_042RO. **A–B**. Holotype (SMF 358976), H 1.31 mm, W 2.11 mm, Ha 0.85 mm. **C–D**. Paratype 1 (SMF 358977), H 1.15 mm, W 2.20 mm, Ha 0.79 mm, Wp 0.20 mm. **E–F**. Paratype 2 (SMF 358978), I19_Ma_85, H 0.68 mm, W 1.47 mm, Ha 0.53 mm, Wp 0.19 mm. — **G–S**. INDEX19_031RO. **G–H**. Paratype 3 (SMF 358979), I19_Ma_86, H 0.84 mm, W 1.48 mm, Ha 0.58 mm. **I–K**. Paratype 4 (SMF 358980), H 0.38 mm, W 0.70 mm, Ha 0.32 mm, Wp 0.20 mm. **L–N**. Paratype 5 (SMF 358981), I19_Ma_80, H 0.86 mm, W 1.34 mm, Wp 0.20 mm. **O–Q**. Paratype 6 (SMF 358982), I19_Ma_81, H 0.72 mm, W 1.30 mm, Wp 0.19 mm. **R–S**. Paratype 7 (SMF 358983), I19_Ma_79, H 0.79 mm, W 1.48 mm, Ha 0.62 mm. Scale bars: 0.1 mm.

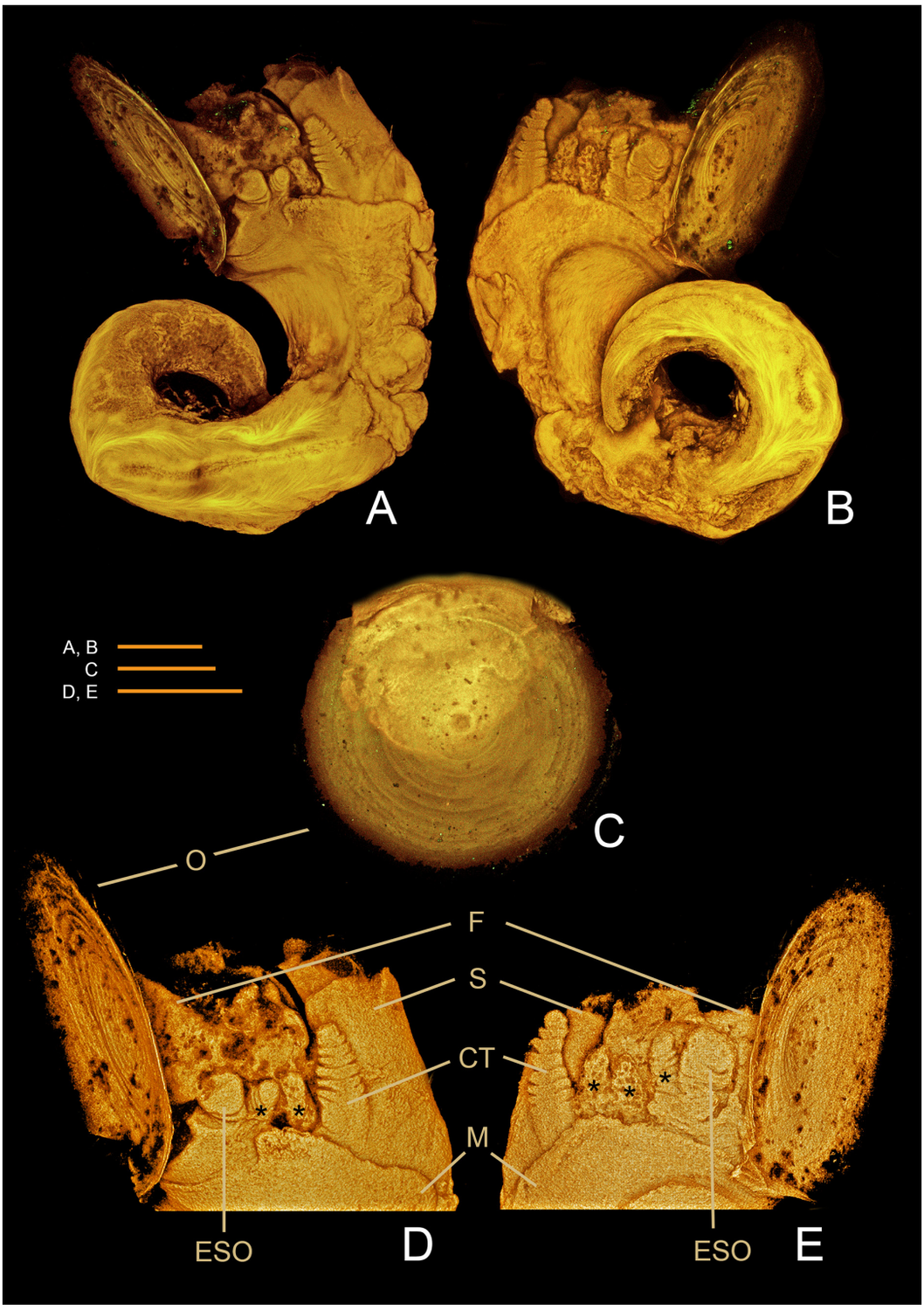

Fig. 4. CLSM images of contracted soft parts of *Anatoma discapex* sp. nov., Central Indian Ridge, INDEX19_042RO, (I19_Ma_83). **A–B**. Complete soft parts in basal and left anterior view (A) and apical and right-anterior view (B). **C**. External view of operculum. **D**. Left anterior view showing cephalic tentacle (CT), epipodial sensory organ (ESO), epipodial appendage (*), foot (F), operculum (O), mantle edge (M) and snout (S). **E**. Right view of anterior with same parts as in D. Scale bars: A–B = 0.2 mm; C = 0.15 mm; D–E = 0.4 mm.

Anatomical description

Snout smooth, broad, flattened with one symmetrical front lobe with pointed front margins on left and right sides (Fig. 4D–E). No eyes observed. Broad cephalic tentacles, tapered, with eight rounded lobes, deeply folded between lobes, gradually decreasing in diameter towards bluntly rounded tip, non-papillate. Foot small when contracted, with irregular surface. Four epipodial appendages on right side; anteriorly two smaller, papillate epipodial tentacles and two large ones posteriorly; the most posterior probably epipodial sensory organ (ESO; Sasaki *et al*. 2010; Haszprunar *et al*. 2017). Three epipodial appendages on left side; small papillate tentacle anteriorly; second smaller epipodial tentacle or small ESO; most posteriorly a large ESO. Visceral mass with little more than one whorl. Mantle smooth with rounded margin, non-papillate.

Operculum (Fig. 4). Yellowish transparent, thin, corneous, multispiral (about 10 whorls) with central nucleus.

Radular teeth. Configuration 30–4–1–4–30; width 0.10 mm. Central tooth broad cusp, directed anteriorly. Four lateral teeth on either side. Inner marginal teeth with multiple large curved hooks on thick stems changing towards external margin into long and thin stems with fine cusps at external margin.

Distribution

Central Indian Ridge, 23–26° S, 69–70° E, depth 2560–3296 m.

Habitat

Living on rocky surface with bacterial mats near active and inactive vents. Shells frequently covered by red bacterial deposit.

Remarks

Shells of *Anatoma discapex* sp. nov. are similar to those of *Anatoma umbilicata* (Jeffreys, 1883), an Atlantic and Mediterranean species from depths of 200–2300 m, *Anatoma parageia* Geiger & Sasaki, 2009 from intertidal zones in eastern Japan and *Anatoma hyposculpta* Geiger, 2012 from the tropical SW Pacific at depths of 730–1620 m (Geiger 2012). All these species show a flattened shoulder but lack the discoid apical outline and the coarse axial sculpture. All other known species in Geiger (2012) have a more elevated spire.

Anatoma declivis sp. nov.

urn:lsid:zoobank.org:act:800FCAD4-D68D-43B9-98A9-209D9C0E0B25

Figs 5–7

Etymology

The species name '*declivis*' refers to the sloping shoulders.

Type material

Holotype

INDIAN OCEAN • CIR; 23.87° S, 69.62° E; depth 2980 m; 12 Nov. 2019; stn INDEX19_033RO; spec. I19_Ma_94, SEM, Fig. 5F–G; SMF 358984.

Paratypes

INDIAN OCEAN • 1 specimen (paratype 1); CIR; 23.88° S, 69.62° E; depth 3082 m; 11 Nov. 2019; stn INDEX19_031RO; spec. I19_Ma_92, SEM, Fig. 5A–C; SMF 358985 • 1 specimen (paratype 2);

same collection data as for preceding; spec. I19_Ma_93, SEM, Fig. 5D–E; SMF 358986 • 1 specimen (paratype 3); CIR; 25.47° S, 69.93° E; depth 2628 m; 16 Nov. 2019; stn INDEX19_042RO, spec. I19_Ma_89, SEM, Fig. 5H–K; SMF 358987 • 1 specimen (paratype 4); SEIR; 27.63° S, 73.87° E; depth 2547 m; 5 Dec. 2019; stn INDEX19_102RO; spec. I19_Ma_87, SEM, Fig. 5L–N; SMF 358988.

Other material examined

INDIAN OCEAN • 1 specimen; CIR; 23.88° S, 69.62° E; depth 3082 m; 11 Nov. 2019; stn INDEX19_031RO; spec. I19_Ma_78 • 4 specimens; CIR; 23.87° S, 69.62° E; depth 2980 m; 12 Nov. 2019; stn INDEX19_033RO; specs I19_Ma_3–4, I19_Ma_6–7 • 3 shells; CIR; 25.47° S, 69.93° E; depth 2934 m; 16 Nov. 2019; INDEX19_042RO • 15 specimens; SEIR; 27.63° S, 73.87° E; depth 2532 m; 5 Dec. 2019; stn INDEX19_102RO; specs I19_Ma_51, I19_Ma_54–61, I19_Ma_63–64, I19_Ma_66–68, I19_Ma_88 • 1 specimen; SEIR; 27.65° S, 73.88° E; depth 2457 m; 11 Dec. 2019; INDEX19_127RO; spec. I19_Ma_77 • 21 specimens; SEIR; 27.65° S, 73.88° E; depth 2469 m; 23 Nov. 2018; stn INDEX18_063RO; specs I18_Ma_256–269, I18_Ma_273–279 • 8 specimens; CIR; 23.78° S, 69.55° E; depth 3049 m; 2 Dec. 2015; stn INDEX15_49R; specs I15_Ma_9, I15_Ma_32, I15_Ma_128–131, I15_Ma_137–138.

Shell description

Protoconch (Fig. 5C of paratype 1). One flat whorl, pointed nucleus, coarsely pitted sculpture; raised sharp lip with smooth flexuous margin at the transition to teleoconch: transition clear by change in sculpture; diameter 0.20 mm.

Teleoconch (Fig. 5F–G). Flattened apex, biconical outline with sloping convex shoulders, protruding margins of selenizone; flexuous axial ribs; round aperture with slit; suture deep. Height 1.19 mm, width 1.90 mm, height of aperture 0.81 mm (67 % of total height); colour opaque grayish white. 2½ regular whorls with convex shoulder area and rounded base, selenizone at periphery; distance between base selenizone and suture minute. Teleoconch I from protoconch to start of selenizone: 0.8–0.9 convex whorls, in plane with protoconch; about 12–25 strong axial ribs, flexuous; no spiral cord. Teleoconch II with selenizone: 20–35 flexuous axial ribs on first whorl, 40–65 ribs on body whorl; ribs at regular spacing, decreasing spacing towards lip. Smooth margins of selenizone sharply protruding upwards, axial ribs weaker and more numerous on external margins; inside margins smooth. Frequency of axial ribs below selenizone slightly higher to that above; rough growth lines between ribs. Base of body whorl shows few spiral cordlets. Umbilicus open, narrow, tortuous and deep; steep spiral keel to centre of columellar callus.

Aperture. Rounded at base, columella, parietal area and shoulder, funnel-shaped at selenizone, pointed at union with penultimate whorl. Lip sharp, flexuous following external ribs, protruding on shoulder area, protruding at columella, thin reclining callus in parietal area. Disk-shaped lower lip; slit at periphery, slit ¼ whorl deep with flattened sharp margins above and below; union of lip aligned with penultimate whorl. Callus thin; inside aperture smooth.

Variation. Little morphological variation of shell. Teleoconch I up to 25 axial ribs, teleoconch II up to 65 axial ribs on body whorl. Base of body whorl occasionally with few spiral cordlets, or with one stronger spiral cord. Adult height range 1.2–1.7 mm; width range 1.9–2.0 mm; H/W ratio range 0.6–0.8. Juvenile shells lower H/W ratio.

Anatomical description

Snout smooth, broad, flattened with two symmetrical front lobes (Fig. 6D–E). No eyes observed. Pair of cephalic tentacles, tapered, with eight rounded lobes, deeply folded between lobes; blunt tip, non-papillate. Foot small in contracted form, with irregular surface. Three epipodial appendages on left side

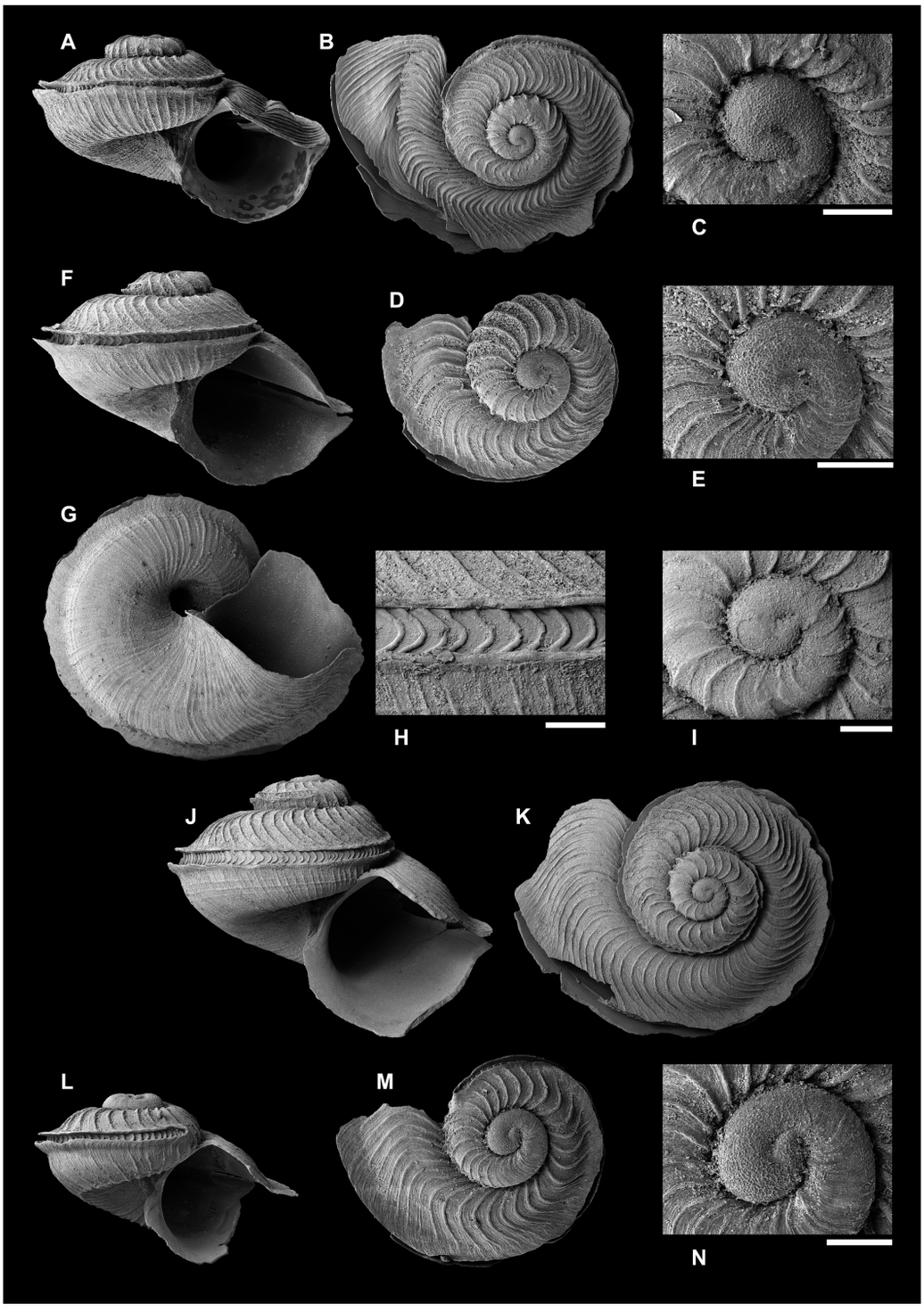

Fig. 5. *Anatoma declivis* sp. nov. **A–C**. Paratype 1 (SMF 358985), I19_Ma_92, INDEX19_031RO, H 1.21, W 1.90 mm, Ha 0.77 mm, Wp 0.19 mm. **D–E**. Paratype 2 (SMF 358986), I19_Ma_93, INDEX19_031RO, W 0.87 mm, Wp 0.20 mm. **F–G**. Holotype (SMF 358984), I19_Ma_94, INDEX19_033RO, H 1.19 mm, W 1.90 mm, Ha 0.81 mm. **H–K**. Paratype 3 (SMF 358987), I19_Ma_89, INDEX19_042RO, H 1.61 mm, W 1.98 mm, Ha 1.00 mm, Wp 0.21 mm. **L–N**. Paratype 4 (SMF 358988), I19_Ma_87, INDEX19_102RO, H 0.63 mm, W 1.00 mm, Ha 0.46 mm, Wp 0.20 mm. Scale bars: 0.1 mm.

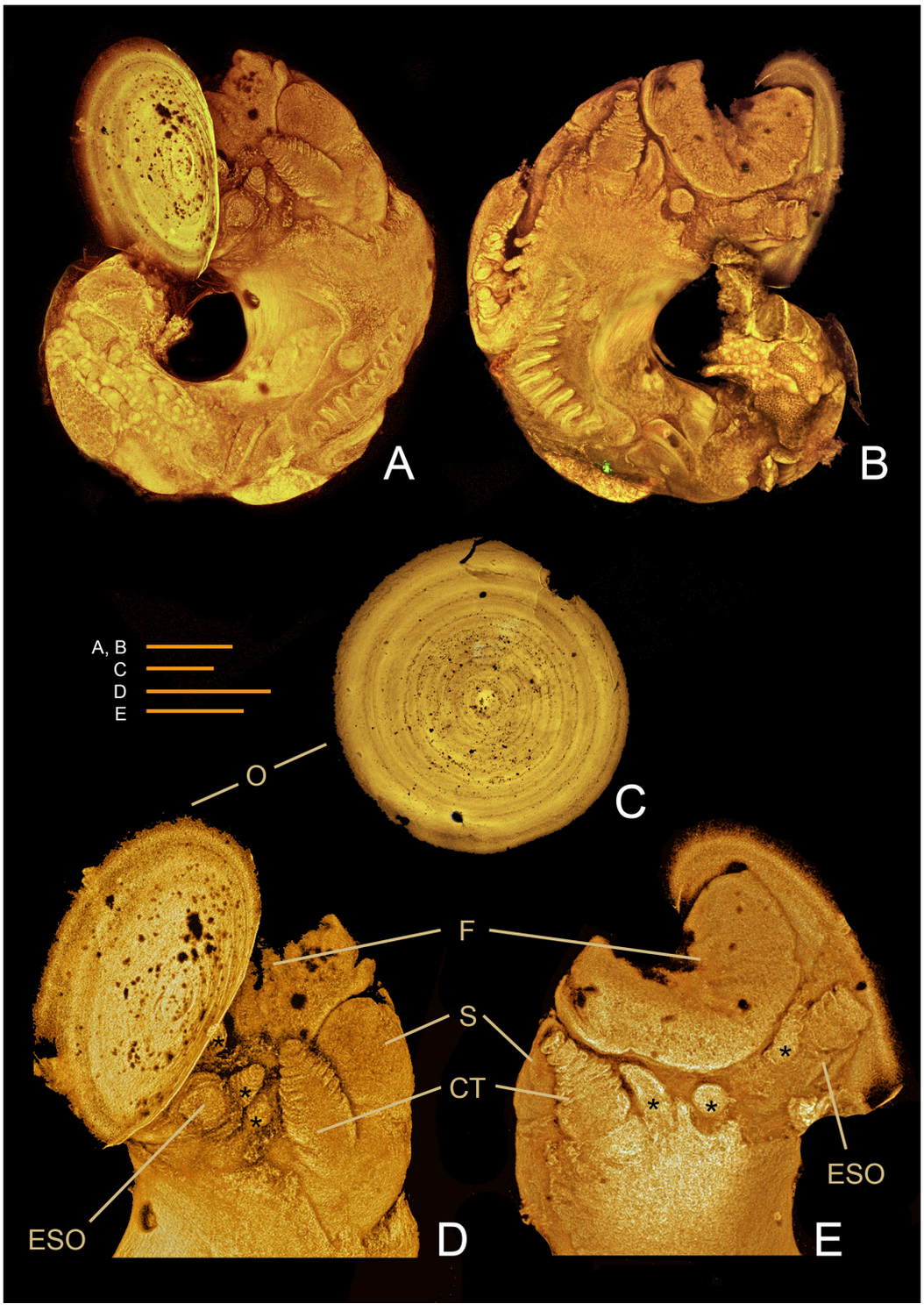

Fig. 6. CLSM images of soft parts of *Anatoma declivis* sp. nov., South-East Indian Ridge, INDEX19_127RO, (I19_Ma_78). **A–B**. Soft parts in basal and left anterior view (A) and apical and right-anterior view; internal tip removed (B). **C**. External view of operculum. **D**. Left anterior view showing cephalic tentacle (CT), epipodial sensory organ (ESO), epipodial appendage (*), foot (F), operculum (O) and snout (S). **E**. Right view of anterior with same parts as in D. Scale bars: A–B = 0.2 mm; C = 0.15 mm; D–E = 0.4 mm.

(Fig. 6D); the two anterior probably epipodial tentacles; ESO posteriorly, non papillate. Four epipodial appendages on right side (Fig. 6E); three epipodial tentacles anteriorly; ESO posteriorly. Mantle smooth.

Operculum. Yellowish transparent, thin, corneous, multispiral (11 whorls) with central nucleus.

Radula (Fig. 7). Largely destroyed in SEM preparation. Central, lateral and marginal teeth arranged 26–4–1–4–26; width 0.15 mm. Central cusped tooth trapezoidal. Four lateral teeth with curved tips. 26 marginal teeth, proximal teeth with 1–3 hooked (curved) denticles (Fig. 7B), distal laterals ending in strongly curved cusp with 6–10 symmetrically-placed, curved denticles (Fig. 7A).

Distribution

Central Indian Ridge and SE Indian Ridge, 23–28° S, 69–74° E, depth 2469–3082 m.

Habitat

Living on rocky surface with bacterial mats near active and inactive vents. Shells are frequently covered by an amorph red bacterial deposit.

Remarks

Shells of *Anatoma declivis* sp. nov. are similar to those of *Anatoma finlayi* (Powell, 1937), an Indo-Pacific species living on the shelf and in bathyal depths, including off Madagascar (Geiger 2012; Table 1). However, the latter species has fine regular spiral cordlets on the teleoconch and its outline is more elevated (H/W 0.8–1.0). All other known species in the Indian Ocean have a stepped outline with a spiral sculpture.

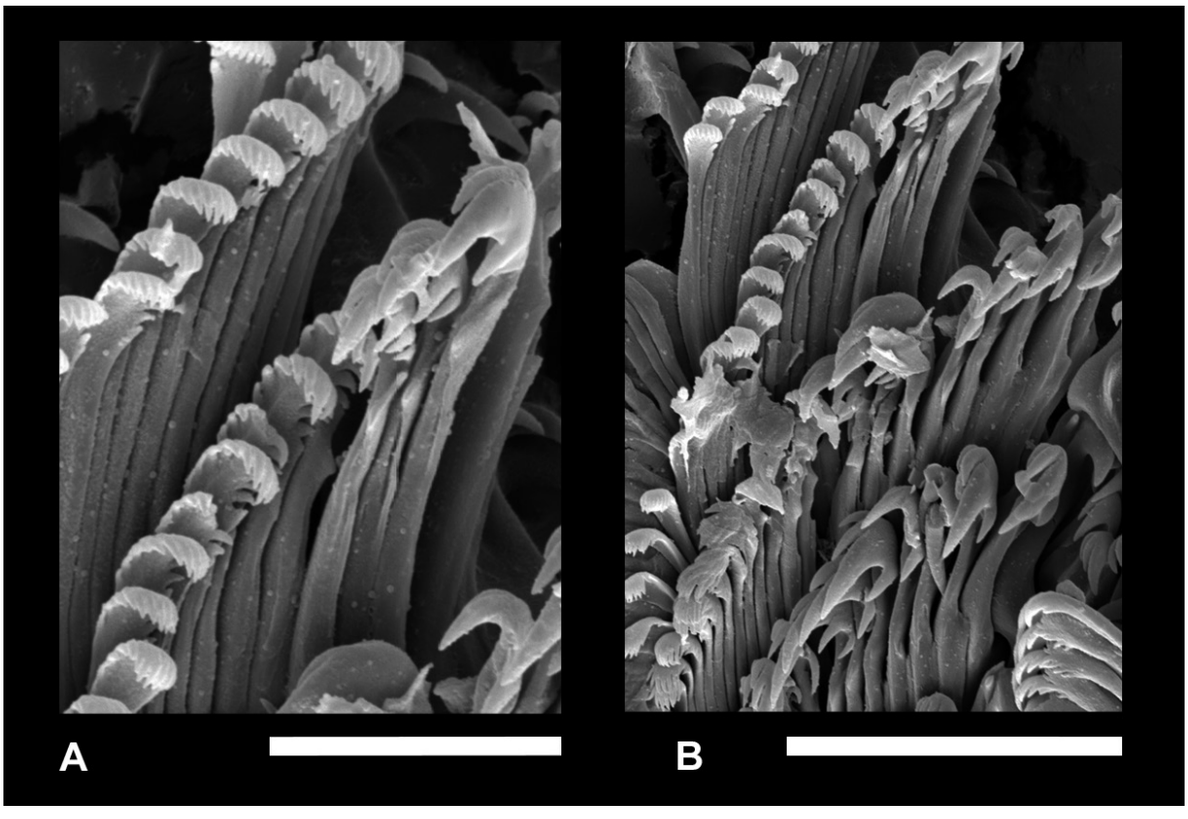

Fig. 7. Radula of *Anatoma declivis* sp. nov., South-East Indian Ridge, INDEX19_127RO, (I19_Ma_78). **A**. SEM image of distal marginal teeth. **B**. SEM image of proximal marginal teeth. Scale bars: 10 μm.

Anatoma laevapex sp. nov.
urn:lsid:zoobank.org:act:FCBC4FC9-05DD-4472-9D3F-336EE8A17002
Figs 8–10

Etymology

The species name '*laevapex*' refers to the smooth initial teleoconch.

Type material

Holotype

INDIAN OCEAN • SEIR; 27.65° S, 73.88° E; depth 2469 m; 11 Dec. 2019; stn INDEX19_127RO; spec. I19_Ma_74, SEM, Fig. 8A–C; SMF 358989.

Paratypes

INDIAN OCEAN • 1 specimen (paratype 1); same location data as for holotype; spec. I19_Ma_75, SEM, Fig. 8D–E; SMF 358990 • 1 specimen (paratype 2); same location data as for holotype; spec. I19_Ma_76, SEM, Fig. 8F–G; SMF 358991.

Other material examined

INDIAN OCEAN • 24 specimens; CIR; 23.87° S, 69.62° E; depth 2980 m; 12 Nov. 2019; stn INDEX19_033RO; specs I19_Ma_8–26, I19_Ma_95–99 • 1 specimen; CIR; 23.78° S, 69.55° E; depth 3049 m; 2 Dec. 2015; INDEX15_49R; spec. I15_Ma_2 • 4 specimens; SEIR; 27.63° S, 73.87° E; depth 2532 m; 5 Dec. 2019; stn INDEX19_102RO; specs I19_Ma_62, I19_Ma_65, I19_Ma_69–70 • 2 specimens; SEIR; 27.65° S, 73.88° E; depth 2469–2471 m; 11 Dec. 2019; stn INDEX19_127RO; specs I19_Ma_72–73.

Shell description

Protoconch (Fig. 8C). One slightly elevated whorl, pointed nucleus, coarsely pitted sculpture; sharp lip with flexuous margin at the transition to teleoconch: transition clear by change in sculpture; diameter 0.19 mm.

Teleoconch (Fig. 8A–B). Flattened spire, disk-shaped outline with sloping weakly convex shoulders, smooth apex, protruding margins of selenizone; flexuous axial ribs; pear-shaped aperture with slit; suture deep. Height 1.0 mm, width 1.5 mm, height of aperture 0.67 mm (67% of total height); colour opaque grayish white. 2¼ regular whorls with convex shoulder area and rounded base, selenizone above periphery; distance between base of selenizone and suture small but increasing regularly. Teleoconch I from protoconch to start of selenizone: one convex whorl, decending below protoconch; smooth, flexuous growth lines; no spiral cord. Teleoconch II with selenizone: 44 regular weak axial ribs on first whorl, last ¼ whorl of body whorl with 17 axial ribs; ribs at regular spacing. Smooth margins of selenizone sharply protruding outwards, axial ribs absent on margins; inside margins smooth. Frequency of axial ribs below selenizone similar to that above; rough growth lines between ribs. Umbilicus open, tortuous and deep; steep spiral keel to base of columellar callus (Fig. 8A of holotype and 8D, F–G of paratypes).

Aperture (Fig. 8B). Rounded base, columella and parietal area; flattened shoulder, funnel-shaped selenizone, pointed union with penultimate whorl. Lip sharp, strongly reclining at union with penultimate whorl, protruding at upper shoulder and columella, thin reclining callus at parietal area; disk-shaped lower lip; slit above periphery, slit ¼ whorl deep with flattened sharp margins above and below. Callus thin; inside aperture smooth.

Variation. Little morphological variation of the shell. 40–50 axial ribs on body whorl. Adult height range 0.9–1.0 mm; width range 1.3–1.5 mm; H/W ratio range 0.65–0.70.

Anatomical description

Body is translucent white anteriorly with orange-brown internal organs in the visceral mass; white radula visible inside translucent neck area. Snout smooth, broad, flattened with two symmetrical lobes in front covered by one flat convex margin on the antero-dorsal part of the snout (Fig. 9D–E). No eyes observed. Pair of broad cephalic tentacles, tapered, with six rounded lobes, deeply folded between lobes, tip blunt, non-papillate. Foot small in contracted form, with irregular surface. Epipodium with five pairs of appendages (Fig. 9D–E). Anteriorly, three pairs of epipodial tentacles or possibly small ESOs,

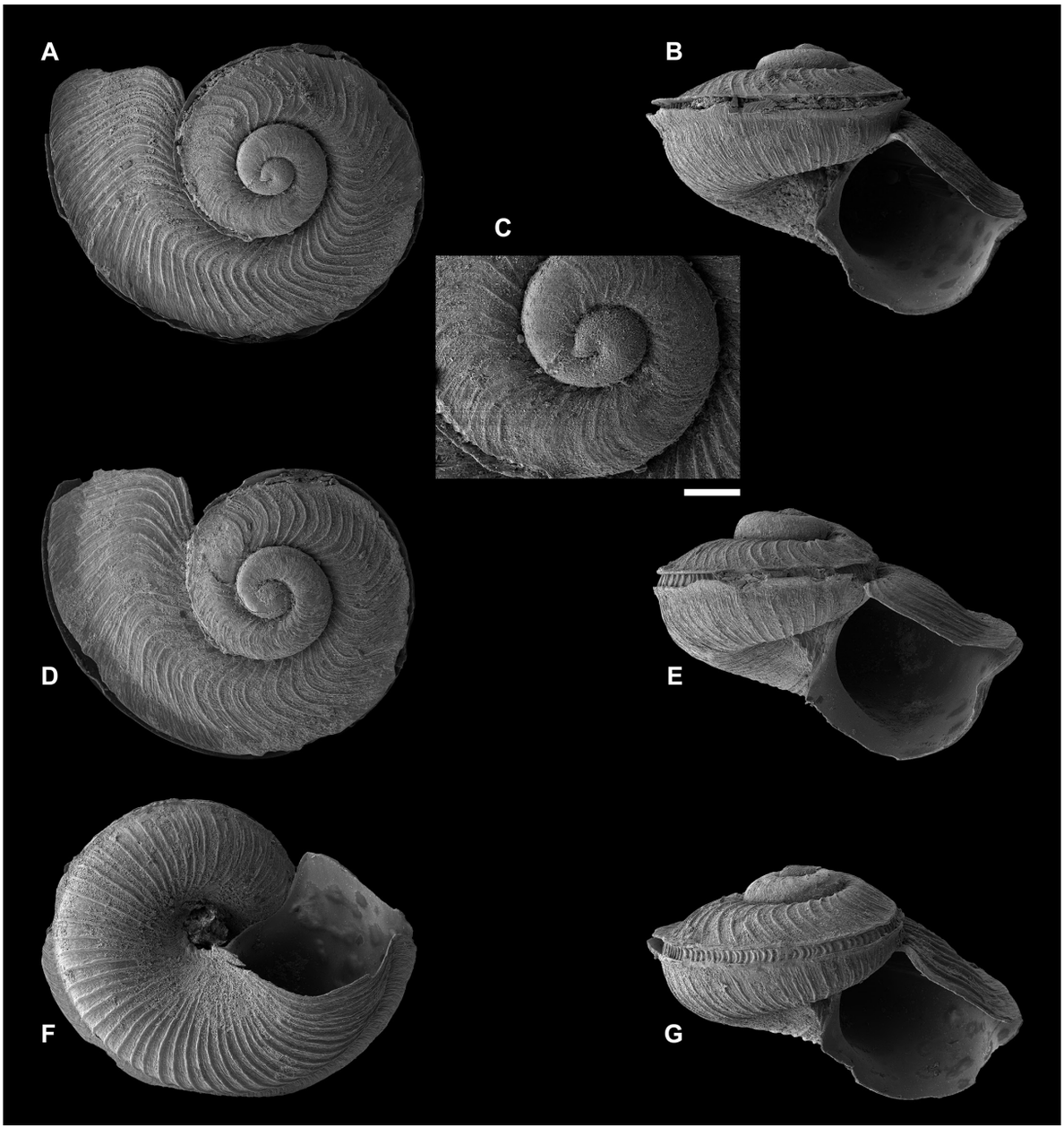

Fig. 8. *Anatoma laevapex* sp. nov. A, G. INDEX19_127RO. **A–C**. Holotype (SMF 358989) (I19_Ma_74) H 1.0 mm, W 1.5 mm, Ha 0.67 mm, Wp 0.19 mm, apical angle 119 deg. **D–E**. Paratype 1 (SMF 358990) (I19_Ma_75) H 0.9 mm, W 1.3 mm, Ha 0.61 mm, Dp 0.19 mm, apical angle 124 deg. **F–G**. Paratype 2 (SMF 358991) (I19_Ma_76) H 0.9 mm, W 1.4 mm, Ha 0.54 mm. Scale bar: 0.1 mm.

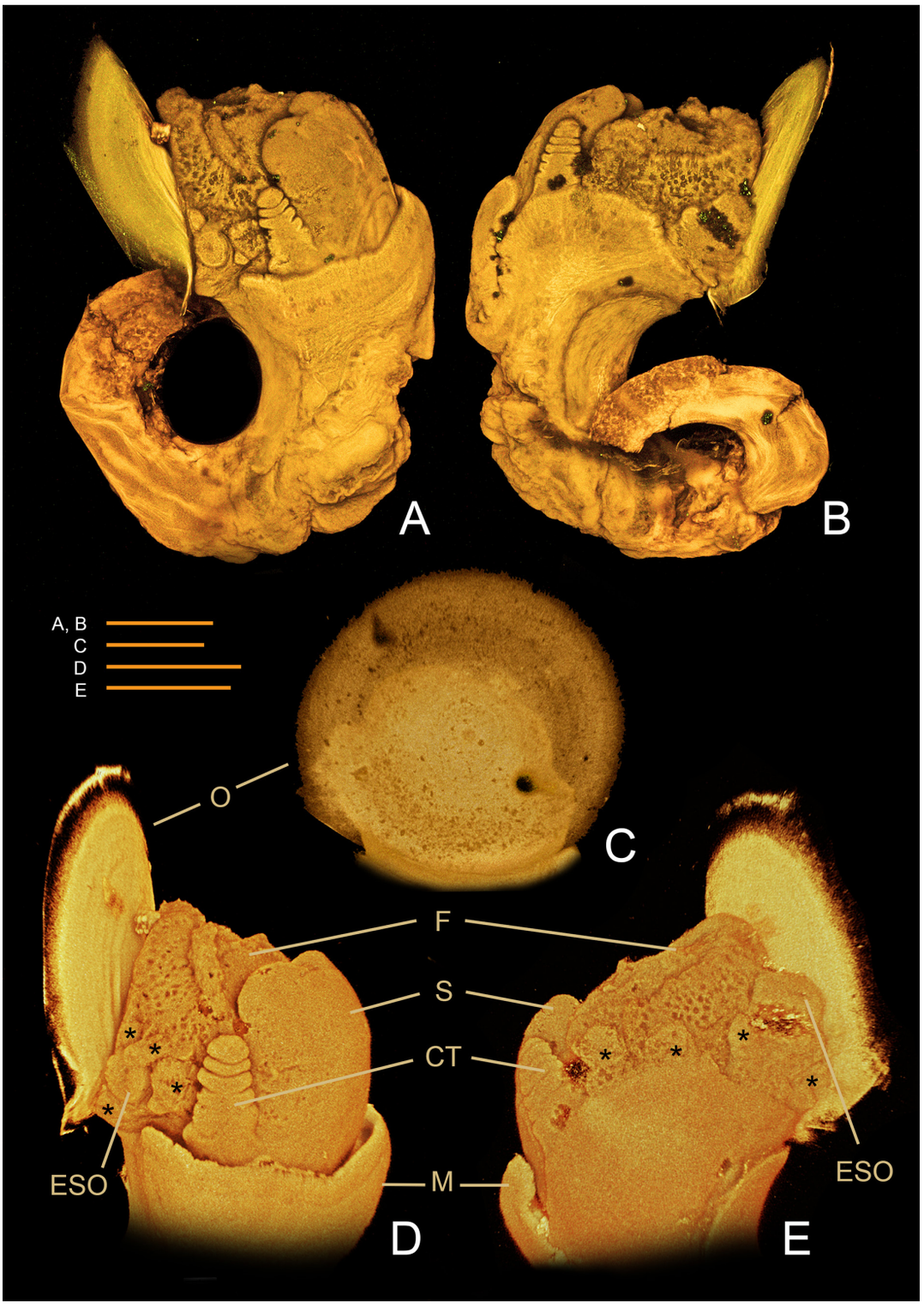

Fig. 9. CLSM images of contracted soft parts of *Anatoma laevapex* sp. nov., INDEX19_127RO (I19_Ma_73). **A–B**. Complete soft parts in apical view (A) and basal view (B). **C**. External view of operculum. **D**. Left antero-dorsal view showing cephalic tentacle (CT), epipodial sensory organ (ESO), epipodial appendage (*), foot (F), operculum (O), mantle edge (M) and snout (S). **E**. Right view of anterior with same parts as in D. Scale bars: 0.5 mm.

marginally papillate. Posteriorly, pair of large ESOs and pair of small epipodial tentacles below the operculum. Mantle smooth with rounded margin, non-papillate.

Operculum (Fig. 9). Yellowish transparent, thin, corneous, multispiral with central nucleus, number of whorls uncertain.

Radula (Fig. 10). With central, lateral and marginal teeth arrangement: 21–4–1–4–21; width 0.15 mm. Central cusped tooth with 5 curved denticles (Fig. 10A), largest central denticle, smaller towards margin; 4 lateral teeth on either side with curved tips and 2 denticles on each tooth, proximal denticle larger than distal denticle; 21 marginal teeth (Fig. 10C), proximal marginal teeth with 1–3 hooked (curved) denticles (Fig. 10E), distal marginal teeth ending in strongly curved cusp with 6–10 symmetrically-placed, curved denticles (Fig. 10D).

Distribution

Central and SE Indian Ridge, 23–28° S, 69–74° E, depth 2469–3049 m.

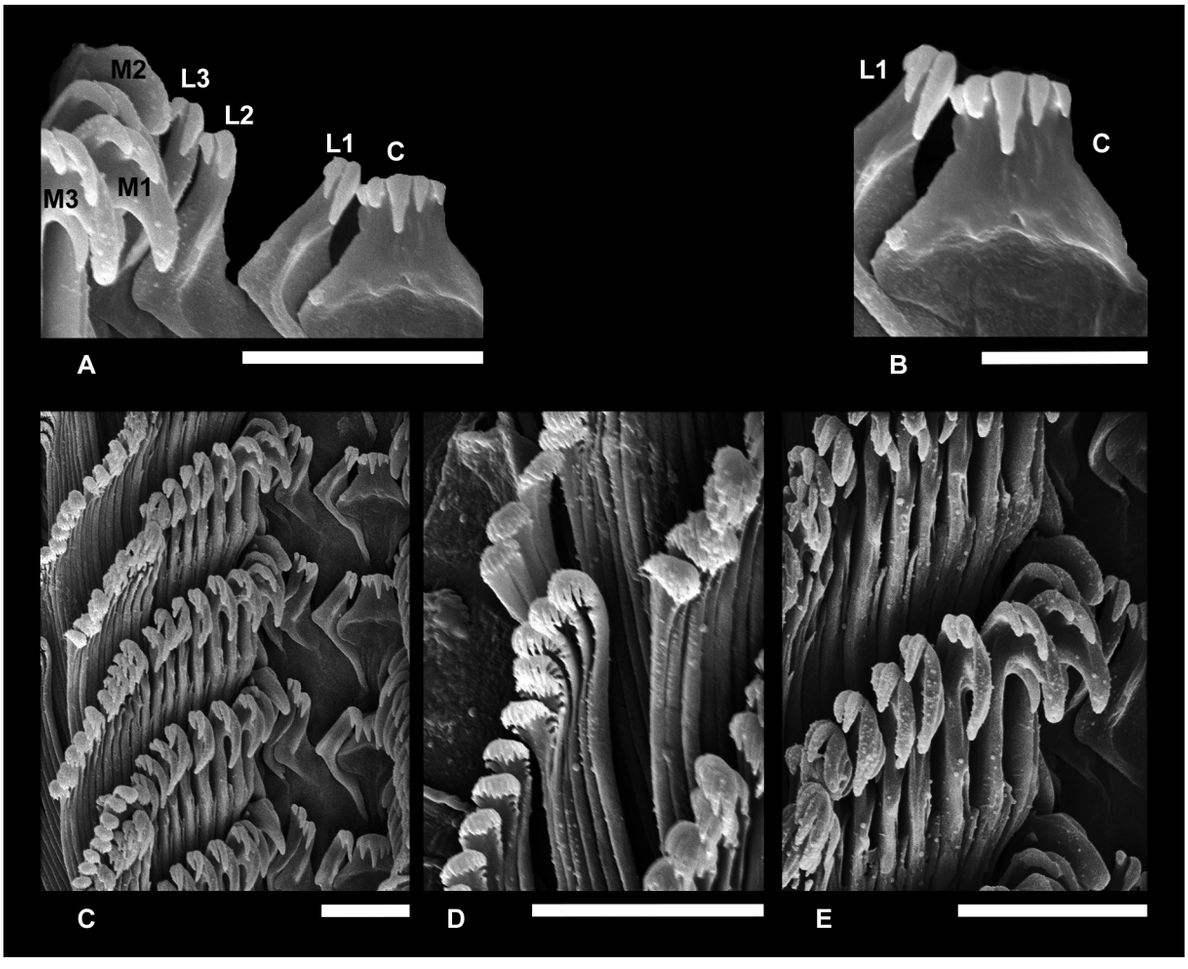

Fig. 10. SEM images of radula of *Anatoma laevapex* sp. nov., I19_033RO (I19_Ma_97). **A**. Central, lateral and inner marginal teeth. **B**. Central and inner lateral teeth. **C**. SEM image of half radula with central, lateral, inner and outer marginal teeth. **D**. Outer marginal teeth. **E**. Inner marginal teeth. Abbreviations: C = central (rachidian) tooth; L1, L2, L3 = inner lateral teeth; M1, M2, M3 = inner marginal teeth. Scale bars: A, C–E = 10 μm; B = 5 μm.

Habitat

Living on rocky surface with bacterial mats near active and inactive vents. Shells frequently covered by red bacterial deposit.

Remarks

Shells, anterior soft parts and radulae of *Anatoma laevapex* sp. nov. are similar to those from *Anatoma declivis* sp. nov. However, the shell of the latter species has fewer and coarser axial ribs including on teleoconch I; its protoconch is sunken. The shell differences with the similar *Anatoma finlayi* (Powell, 1937) and other known species in the Indian Ocean are mentioned under the remarks of *Anatoma declivis* sp. nov.

Anatoma pauciculpta sp. nov.

urn:lsid:zoobank.org:act:337D20DA-8BE8-4C69-82A1-8EE444B72C48

Fig. 11

Etymology

The species name '*pauciculpta*' refers to the inconspicuous sculpture on the shell.

Type material

Holotype

INDIAN OCEAN • CIR; 23.88° S, 69.62° E; depth 3296 m; 8 Dec. 2015; stn INDEX15_62R; spec. I15_Ma_169, SEM, Fig. 11D–H; SMF 358992.

Paratypes

INDIAN OCEAN • 1 juvenile shell; SEIR; 27.63° S, 73.87° E; depth 2618 m; 6 Dec. 2019; stn INDEX19_104RO; spec. I19_Ma_91, SEM, Fig. 11A–C; SMF 358993.

Other material examined

INDIAN OCEAN • 2 specimens; SEIR; 27.63° S, 73.87° E; depth 2532–2621 m; 7 Dec. 2019; stn INDEX19_106RO; specs I19_Ma_52, I19_Ma_71 • 2 specimens; SEIR; 27.65° S, 73.88° E; depth 2469 m; 23 Nov. 2018; stn INDEX18_063RO; specs I18_Ma_271–272.

Shell description

Protoconch (Fig. 11F). One slightly elevated whorl, evenly rounded, sculpture small, irregularly oriented, straight or curved, short ridges; few spiral striae; smooth straight rim near margin; sharp flexuous lip, protrusion at periphery; transition to teleoconch clear by change in sculpture; diameter 0.21 mm.

Teleoconch (Fig. 11D–E). With elevated spire, swollen whorls with protruding margins of selenizone; with spiral cordlets; rounded aperture with slit; suture deep. Height 1.0 mm, width 1.2 mm, height of aperture 0.7 mm (70 % of total height); colour translucent grayish white. 2¼ regular whorls with convex shoulder area and rounded base, selenizone slightly above periphery. Teleoconch I from protoconch to start of selenizone: slightly more than one well-rounded whorl, descending below protoconch; smooth, with up to six spiral cordlets, numerous prosocline growth lines. Teleoconch II with selenizone: slightly more than one whorl; shoulder area with seven spiral cordlets at the lip margin; new weaker cordlets emerging between older ones. Margins of selenizone sharply protruding outwards; growth lines on external sides of selenizone; inside margins smooth; surface between margins smooth with curved growth lines (Fig. 11B, E, H). Base body whorl smooth background with about 20 irregularly spaced

spiral cordlets and about 60 regular axial riblets; spiral and axial sculpture stronger in umbilical area (Fig. 11G).

Umbilicus. Open, tortuous and deep; steep smoothly curved spiral keel ending at base of columellar callus (Fig. 11D, G).

Aperture (Fig. 11D). With semi-circular rounded base, funnel-shaped towards selenizone, convex shoulder, pointed at union with penultimate whorl, well rounded on parietal and columellar side. Lip sharp; protruding, oblique on columella with minor rib joining in v-shape with columellar keel (Fig. 11G); rounded towards base and parietal area with thin callus. Slit ¼ whorl deep with flattened sharp margins above and below, lip prosocline, union perpendicular to penultimate whorl (Fig. 11E). Callus thin; inside aperture smooth.

Anatomical description

Animal unknown; the soft parts of the live-collected specimen have been used for molecular analyses or retained in ethanol for future studies.

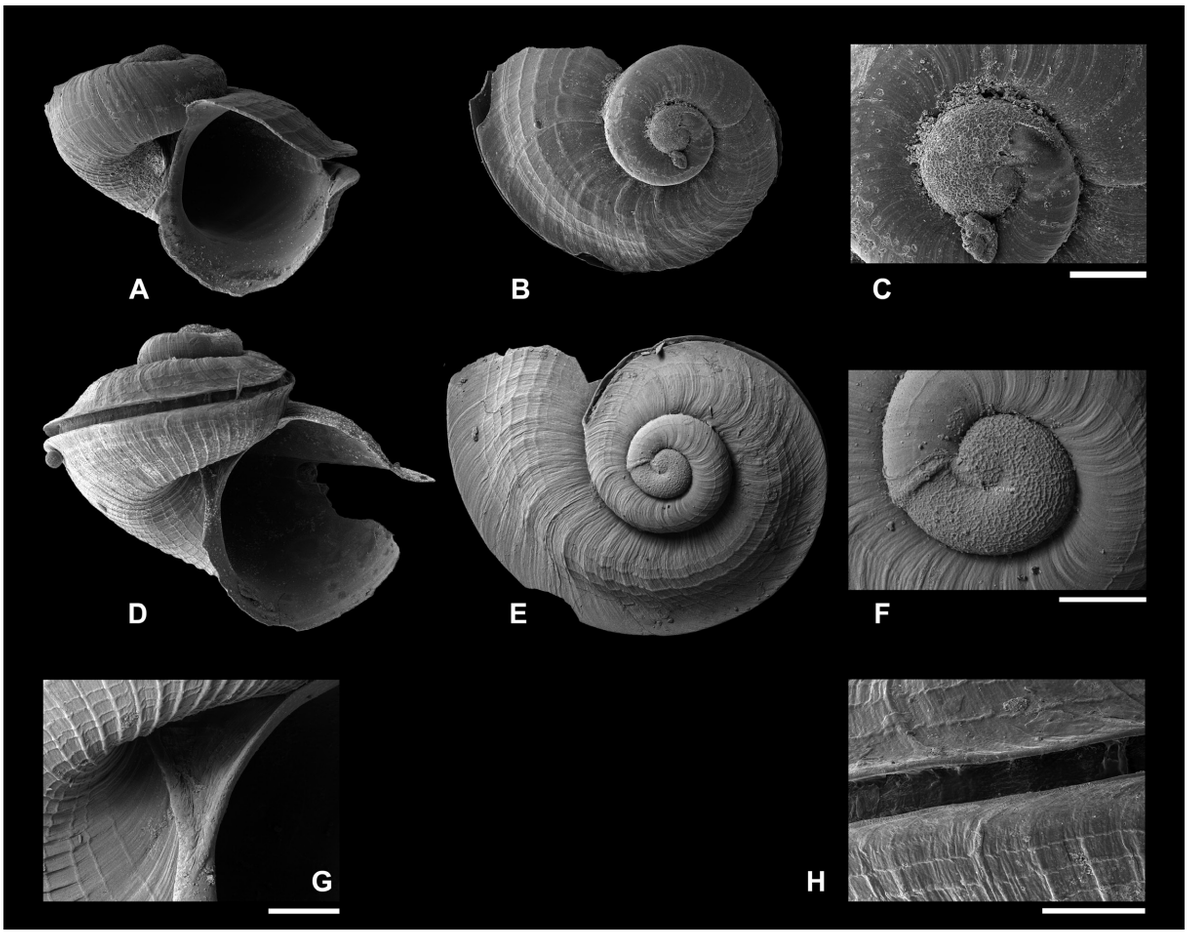

Fig. 11. *Anatoma pauciculpta* sp. nov. **A–C**. Paratype (SMF 358993), INDEX19_104RO (I19_Ma_91). H 0.77 mm, W 0.99 mm, Ha 0.61 mm, Wp 0.20 mm. **D–H**. Holotype (SMF 358992), INDEX15_62R (I15_Ma_169), H 1.03 mm, W 1.20 mm, Ha 0.70 mm, Wp 0.21 mm. Scale bars: 0.1 mm.

Habitat

Living on rocky surface with bacterial mats near active and inactive vents.

Distribution

Central and SE Indian Ridge, 23–28° S, 69–74° E, depth 2469–3296 m.

Remarks

The lack of distinct and regular spiral and or axial sculpture is uncommon. The outline is similar to that of *Anatoma africanae* (Herbert, 1963) from the Gallieni Fracture Zone, south of Madagascar at a depth of 400 m, but this species has a distinct and fine axial and spiral sculpture.

Discussion

To date, thirteen species in Anatomidae were known from the Indian Ocean, most with a shelf to bathyal range (Geiger 2012; Table 1). Only two species were found alive at depths of 2500–3000 m (Geiger 2012): *Anatoma munieri* (Fischer, 1862) and *Anatoma porcellana* Geiger 2012, both found at a considerable distance from the investigated areas in this study and morphologically different from the new species presented. The identification of six species from the Central Indian Ridge and SE Indian Ridge gives testimony to the unique variability in habitats and related malaco-diversity in this relatively small area of the Indian Ocean. The four newly described species are considered endemic to the vent areas in the central Indian Ocean.

Three newly described species are distributed over an 800 km long trajectory along the central Indian plate margins: *Anatoma declivis* sp. nov., *Anatoma laevapex* sp. nov. and *Anatoma pauciculpta* sp. nov. *Anatoma discapex* sp. nov. has only been found on the Central Indian Ridge near the Rodriguez Triple Junction. The simple protoconchs indicate a direct larval development or a short lecitotrophic phase. It is yet unclear how they are capable of crossing abyssal gaps without food supply; this paradox is shared with many other Vetigastropods (Hoffman *et al*. 2021 and references therein).

The radulae in three investigated new species have simple cusped central teeth and lateral teeth with few denticles, inner marginal teeth with large, curved hooks with up to four denticles and outer marginal teeth with stilted cusps with many denticles. The number of marginal teeth varies among these three species between 21 and 30. *Anatoma discapex* sp. nov. had the highest number of marginal teeth (30) in a relatively narrow teeth-row (0.10 mm) when compared to *Anatoma declivis* sp. nov. (26 marginal teeth; row width 0.15 mm) or *Anatoma laevapex* sp. nov. (21 marginal teeth; row width 0.15 mm). Similar radulae were observed in *Anatoma agulhasensis* (Thiele, 1925), a species from the upper shelf of Africa (Geiger 2012: 749, fig. 602). *Anatoma biconica* Geiger, 2012 from bathyal depths in the southern Indo-Pacific (including off S Madagascar) has more denticles on the central and inner marginal teeth (Geiger 2012: 815, fig. 658). *Anatoma flexidentata* Geiger & Sasaki, 2008 is an abyssal Indo-Pacific species described from nearby Réunion (3300–3240 m) with completely different radular morphology with serrated pointed central teeth and curved denticles as outer marginal teeth (Geiger 2012: 892, fig. 719). The Indo-Pacific *Anatoma japonica* (Adams, 1862) is also found at upper bathyal depths off Madagascar and Réunion; it has similar central teeth but more serrated inner marginal teeth (Geiger 2012: 935, fig. 759). *Anatoma porcellana* Geiger, 2012 is an Indo-Pacific species, which has been found in bathyal depths off S Madagascar; its central and inner marginal teeth are similar but more serrated than those of our new species (Geiger 2012: 1023, fig. 892). *Anatoma janetae* Geiger, 2006 from 2567–2606 m on the East Pacific Rise also has a similar rachidian (central) tooth, lateral teeth and inner marginal teeth but it has different outer marginal teeth (Geiger 2006: fig. 3).

The morphologies of the anterior soft parts of three new species are similar. All cephalic tentacles have a tapered outline, non-papillate with multple lobes. Geiger (2012) imaged cephalic tentacles of some hitherto known *Anatoma*; they show an elongated shape with many tiny papillae; for example, the Antarctic *Anatoma euglyptae* (Pelseneer, 1903) and *A. weddelliana* (Zelaya & Geiger, 2007), the Japanese *A. fujikurai* Sasaki, Geiger & Okutani, 2010, the W American *A. kelseyi* (Dall, 1905) and *A. janetae* Geiger, 2006, the Peruvian *A. peruviana* (Geiger & McLean, 2010) and the NE Atlantic *A. tenuisculpta* (Seguenza, 1877). Haszprunar *et al*. (2017) studied the epipodial and cephalic appendages in basal gastropods. They confirmed that ESO pairs are present in species in Cocculiniformia, Neomphalida and Vetigastropoda. Species in Scissurellidae (Vetigastropoda) showed a pair of papillate cephalic tentacles, one or two pairs of papillate epipodial tentacles and one ESO pair. Species in Scissurellidae are considered closely related to Anatomidae. Geiger (2006: fig. 2) indicates several pairs of epipodial tentacles on *Anatoma janetae*; his image does not allow confirmation of one or more ESO pairs. Our observations indicate a posterior non-papillate pair of ESOs in three new vent species. Up to four pairs of epipodial tentacles and/or additional ESO pairs have been observed. Some epipodial tentacles seem papillate. The cephalic tentacles of three new species are elongate, tapered, strongly lobed and non-papillate.

It is likely that anatomical traits of anatomids were adapted to food type available in the abyssal vent habitats. We presume an oligotrophic environment for all habitats; high oxygen concentration but little falling detritus. Nevertheless, the mineral-rich habitat is ideal for a bloom in Bacteria and Archaea (Han *et al*. 2018), which likely provide food for small vetigastropods. Many specimens are covered by a red deposit, probably containing bacteria. Different mineral environments will yield different Bacteria and Archaea, which might enhance the introduction of different species.

Switching on and off of food supplies by changes in mineral output across the oceanic plate margins in recent geological times will enhance distribution as well as isolation of new species. The genetic divergence of various species is probably associated with a morphological divergence: *Anatoma laevapex* sp. nov. and *A. declivis* sp. nov. are morphologically very similar, followed by *A. discapex* sp. nov. In contrast, the COI sequences of *Anatoma laevapex* sp. nov. and *A. discapex* sp. nov. are similar, with *A. declivis* sp. nov. being more distant. *Anatoma pauciculpta* sp. nov. shows greater differences in shell morphology and COI sequence. A relatively large COI distinctness is also observed in the two additional MOTUs.

Genetic and morphological divergence is expected to increase with increasing linear distance along the plate margins. Future sampling could be extended North, SE and SW to establish the limits of the species ranges. Moreover, a possible relationship between different types of bacterial mats and anatomid species could indicate different or preferred food sources for species.

A systematic analysis on the occurrence of anatomids in other plate margin areas has not been done to date; most studies were done on the Mid Atlantic Ridge (MAR) and the East Pacific Rise (EPR). *Anatoma tenuis* (Jeffreys, 1877) was originally described near the MAR at a depth of 2521 m but the species has also been found on the North Atlantic abyssal plane at depths of 5500–5987 m as was the synonymous *A. josephinae* Odhner, 1960 (Geiger 2012). *Anatoma umbilicata* (Jeffreys, 1883) has been found on the MAR around the Azores but this species is widely distributed in the NE Atlantic Ocean and into the Mediterranean Sea (Geiger 2012). *Anatoma aspera* (Philippi, 1844) and *A. tenuisculpta* (Seguenza, 1877) have been found on the northern MAR south-west of Iceland at depths of 242–321 m (unpublished records from the reference collection at SaM). These latter species have a wide NE Atlantic and Mediterranean distribution range (Geiger 2012). Therefore, the anatomids known from the MAR cannot be regarded as typical vent fauna. *Anatoma janetae* Geiger, 2006 is the only anatomid orginally reported on the EPR from 2567–2606 m depth (Geiger 2006: 108). More recent records (Geiger 2012:

922) also report *A. janetae* in 850–900 m depth off the northwestern USA. In summary, the new anatomids on the plate margins in the Indian Ocean are solely known as endemic vent fauna. To date, anatomids known from MAR and EPR are not restricted to plate margin habitats and they have shown more extensive distribution areas.

Acknowledgements

We thank Dr Thomas Kuhn, current chief-scientist of the INDEX exploration program, Dr Ulrich Schwarz-Schampera, former chief-scientist of the INDEX exploration program during the INDEX 2015, INDEX 2018 and INDEX 2019 cruises; the captains, crews and scientific staff of R/V *Pelagia* and R/V *Sonne* for their assistance in the cruises; the pilots and technicians of ROV ROPOS for their dedication in studying the vent fields and collecting the samples that enabled this study. The study was funded by the INDEX exploration project for marine polymetallic sulphides by the Federal Institute for Geosciences and Natural Resources (BGR) on behalf of the German Federal Ministry for Economic Affairs and Energy. Exploration activities are carried out in the framework and under the regulations of an exploration license with the International Seabed Authority. This is publication number 62 that uses data from the Senckenberg am Meer Confocal Laser Scanning Microscope Facility and publication number 88 from the Metabarcoding and Molecular Laboratory. We are grateful to anonymous editors for improving our manuscript.

References

Altschul S.F., Gish W., Miller W., Myers E.W. & Lipman D.J. 1990. Basic local alignment search tool. *Journal of Molecular Biology* 215: 403–410. https://doi.org/10.1016/S0022-2836(05)80360-2

Chen C., Copley J.T., Linse K., Rogers A.D. & Sigwart J.D. 2015a. The heart of a dragon: 3D anatomical reconstruction of the 'scaly-foot gastropod' (Mollusca: Gastropoda: Neomphalina) reveals its extraordinary circulatory system. *Frontiers in Zoology* 12 (1): 13. https://doi.org/10.1186/s12983-015-0105-1

Chen C., Linse K., Copley J.T. & Rogers A.D. 2015b. The 'scaly-foot gastropod': a new genus and species of hydrothermal vent-endemic gastropod (Neomphalina: Peltospiridae) from the Indian Ocean. *Journal of Molluscan Studies* 81 (3): 322–334. https://doi.org/10.1093/mollus/eyv013

Chen C., Uematsu K., Linse K. & Sigwart J.D. 2017. By more ways than one: rapid convergence at hydrothermal vents shown by 3D anatomical reconstruction of *Gigantopelta* (Mollusca: Neomphalina). *BMC Evolutionary Biology* 17 (1): 1–19. https://doi.org/10.1186/s12862-017-0917-z

Chen C., Han Y., Copley J.T. & Zhou Y. 2021. A new peltospirid snail (Gastropoda: Neomphalida) adds to the unique biodiversity of Longqi vent field, Southwest Indian Ridge. *Journal of Natural History* 55 (13–14): 851–866. https://doi.org/10.1080/00222933.2021.1923851

Galindo L., Puillandre N., Strong E. & Bouchet P. 2014. Using microwaves to prepare gastropods for DNA Barcoding. *Molecular Ecology Resources* 14: 700–705. https://doi.org/10.1111/1755-0998.12231

Geiger D.L. 2006. A new blind *Anatoma* species from the bathyal of the northeastern Pacific (Vetigastropoda: Anatomidae). *Molluscan Research* 26 (2): 108–112.

Geiger D.L. 2012. *Monograph of the Little Slit Shells. Volume 1. Introduction, Scissurellidae*: 1–728. *Volume 2. Anatomidae, Larocheidae, Depressizonidae, Sutilizonidae, Temnocinclidae*: 729–1291. Santa Barbara Museum of Natural History Monographs 7, Santa Barbara.

Geiger D.L. & Thacker C. 2005. Molecular phylogeny of Vetigastropoda reveals non-monophyletic Scissurellidae, Trochoidea, and Fissurelloidea. *Molluscan Research* 25: 47–55.

Geller J., Meyer C., Parker M. & Hawk H. 2013. Redesign of PCR primers for mitochondrial cytochrome c oxidase subunit I for marine invertebrates and application in all-taxa biotic surveys. *Molecular Ecology Resources* 13: 851–861. https://doi.org/10.1111/1755-0998.12138

Gerdes K.H., Martínez Arbizu P., Schwarz-Schampera U., Schwentner M. & Kihara T.C. 2019a. Detailed mapping of hydrothermal vent fauna: a 3D reconstruction approach based on video imagery. *Frontiers in Marine Science* 6: 96. https://doi.org/10.3389/fmars.2019.00096

Gerdes K.H., Martínez Arbizu P., Schwentner M., Freitag R., Schwarz-Schampera U., Brandt A. & Kihara T.C. 2019b. Megabenthic assemblages at the southern Central Indian Ridge–spatial segregation of inactive hydrothermal vents from active-, periphery-and non-vent sites. *Marine Environmental Research* 151: 104776. https://doi.org/10.1016/j.marenvres.2019.104776

Gerdes K.H., Kihara T.C., Martínez Arbizu P., Kuhn T., Schwarz-Schampera U., Mah C.L., Norenburg J.L., Linley T.D., Shalaeva K., Macpherson E., Gordon D., Stöhr S., Messing C.G., Bober S., Guggolz T., Christodoulou M., Gebruk A., Kremenetskaia A., Kroh A., Sanamyan K., Bolstad K., Hoffman L., Gooday A.J. & Molodtsova T. 2021. Megafauna of the German exploration licence area for seafloor massive sulphides along the Central and South East Indian Ridge (Indian Ocean). *Biodiversity Data Journal* 9: e69955. https://doi.org/10.3897/BDJ.9.e69955

Han Y., Gonnella G., Adam N., Schippers A., Burkhardt L., Kurtz S., Schwarz-Schampera U., Franke H. & Perner M. 2018. Hydrothermal chimneys host habitat-specific microbial communities: analogues for studying the possible impact of mining seafloor massive sulfide deposits. *Scientific Reports* 10386. https://doi.org/10.1038/s41598-018-28613-5

Hashimoto J., Ohta S., Gamo T., Chiba H., Yamaguchi T., Tsuchida S., Okudaira T., Watabe H., Yamanaka T. & Kitazawa M. 2001. First hydrothermal vent communities from the Indian Ocean discovered. *Zoological science* 18 (5): 717–721. https://doi.org/10.2108/zsj.18.717

Haszprunar G., Kunze T., Warén A. & Heß M. 2017. A reconsideration of epipodial and cephalic appendages in basal gastropods: homologies, modules and evolutionary scenarios. *Journal of Molluscan Studies* 83 (4): 363–383. https://doi.org/10.1093/mollus/eyx032

Hoffman L., Gofas S. & Freiwald A. 2021. The genus *Anatoma* Woodward, 1859 (Gastropoda, Anatomidae) from Azorean seamounts collected during the R/V Meteor Cruise M151 Athena. *Iberus* 39 (2): 139–152. https://doi.org/10.5281/zenodo.5035715

Johnson S.B., Warén A., Tunnicliffe V., van Dover C., Wheat C.G., Schultz T.F. & Vrijenhoek R.C. 2015. Molecular taxonomy and naming of five cryptic species of *Alviniconcha* snails (Gastropoda: Abyssochrysoidea) from hydrothermal vents. *Systematics and Biodiversity* 13 (3): 278–295. https://doi.org/10.1080/14772000.2014.970673

Kano Y. 2008. Vetigastropod phylogeny and a new concept of Seguenzioidea: independent evolution of copulatory organs in the deep-sea habitats. *Zoologica Scripta* 37: 1–21. https://doi.org/10.1111/j.1463-6409.2007.00316.x

Katoh K., Misawa K., Kuma K. & Miyata T. 2002. MAFFT: a novel method for rapid multiple sequence alignment based on fast Fourier transform. *Nucleic Acids Researh* 30: 3059–3066. https://doi.org/10.1093/nar/gkf436

Kearse M., Moir R., Wilson A., Stones-Havas S., Cheung M., Sturrock S., Buxton S., Cooper A., Markowitz S., Duran C., Thierer T., Ashton B., Meintjes P. & Drummond A. 2012. Geneious Basic: an integrated and extendable desktop software platform for the organization and analysis of sequence data. *Bioinformatics* 28 (12):1647–1649. https://doi.org/10.1093/bioinformatics/bts199

Kim J., Son S.K., Kim D., Pak S.J., Yu O.H., Walker S.L., Oh J., Choi S.K., Ra K., Ko Y. & Kim K.H. 2020. Discovery of active hydrothermal vent fields along the Central Indian Ridge, 8–12°S. *Geochemistry, Geophysics, Geosystems* 21 (8): e2020GC009058. https://doi.org/10.1029/2020GC009058

Kumar S., Stecher G., Li M., Knyaz C. & Tamura K. 2018. MEGA X: Molecular Evolutionary Genetics Analysis across computing platforms. *Molecular Biology Evolution* 35: 1547–1549. https://doi.org/10.1093/molbev/msy096

Li W. & Godzik A. 2006. Cd-hit: a fast program for clustering and comparing large sets of protein or nucleotide sequences. *Bioinformatics* 22 (13): 1658–1659. https://doi.org/10.1093/bioinformatics/btl158

Lobo Arteaga J., Costa P., Teixeira M., Ferreira M., Costa M.H. & Costa F. 2013. Enhanced primers for amplification of DNA barcodes from a broad range of marine metazoans. BMC *Ecology* 13: 34. https://doi.org/10.1186/1472-6785-13-34

Monaghan M.T., Wild R., Elliot M., Fujisawa T., Balke M., Inward D.J.G., Lees D.C., Ranaivosolo R., Eggleton P., Barraclough T.G. & Vogler A.P. 2009. Accelerated species inventory on Madagascar using coalescent-based models of species delineation. *Systematic Biology* 58 (3): 298–311. https://doi.org/10.1093/sysbio/syp027

Nakamura K., Watanabe H., Miyazaki J., Takai K., Kawagucci S., Noguchi T., Nemoto S., Watsuji T.O., Matsuzaki T., Shibuya T. & Okamura K. 2012. Discovery of new hydrothermal activity and chemosynthetic fauna on the Central Indian Ridge at 18–20° S. *PLoS ONE* 7 (3): e32965. https://doi.org/10.1371/journal.pone.0032965

Okutani T., Hashimoto J. & Sasaki T. 2004. New gastropod taxa from a hydrothermal vent (Kairei Field) in the Central Indian Ocean. *Venus* 63: 1–11.

Pons J., Barraclough T.G., Gomez-Zurita J., Cardoso A., Duran D.P., Hazell S., Kamoun S., Sumlin W.D. & Vogler A.P. 2006. Sequence-based species delimitation for the DNA taxonomy of undescribed insects. *Systematic Biology* 55 (4): 595–609. https://doi.org/10.1080/10635150600852011

Puillandre N., Lambert A., Brouillet S. & Achaz G. 2012. ABGD, Automatic Barcode Gap Discovery for primary species delimitation. *Molecular Ecology* 21: 1864–1877. https://doi.org/10.1111/j.1365-294X.2011.05239.x

Ratnasingham S. & Hebert P.D.N. 2007. BOLD: the Barcode of Life Data System (http://www.barcodinglife.org). *Molecular Ecology Notes* 7: 355–364. https://doi.org/10.1111/j.1471-8286.2007.01678.x

Ratnasingham S. & Hebert P.D.N. 2013. A DNA-based registry for all animal species: the Barcode Index Number (BIN) system. *PLoS ONE* 8: e66213. https://doi.org/10.1371/journal.pone.0066213

Sasaki T., Geiger D.L. & Okutani T. 2010. A new species of *Anatoma* (Vetigastropoda: Anatomidae) from a hydrothermal vent field in Myojin Knoll Caldera, Izu-Ogasawara Arc, Japan. *Veliger* 51 (1): 63–75.

Suchard M.A., Lemey P., Baele G., Ayres D.L., Drummond A.J. & Rambaut A. 2018. Bayesian phylogenetic and phylodynamic data integration using BEAST 1.10. *Virus Evolution* 4 (1): vey016. https://doi.org/10.1093/ve/vey016

Sun J., Zhou Y., Chen C., Kwan Y.H., Sun Y., Wang X., Yang L., Zhang R., Wei T., Yang Y. & Qu L. 2020. Nearest vent, dearest friend: biodiversity of Tiancheng vent field reveals cross-ridge similarities in the Indian Ocean. *Royal Society Open Science* 7 (3): 200110. https://doi.org/10.1098/rsos.200110

Van Dover C.L. 2002. Trophic relationships among invertebrates at the Kairei hydrothermal vent field (Central Indian Ridge). *Marine Biology* 141 (4): 761–772. https://doi.org/10.1007/s00227-002-0865-y

Van Dover C.L., Humphris S.E., Fornari D., Cavanaugh C.M., Collier R., Goffredi S.K., Hashimoto J., Lilley M.D., Reysenbach A.L., Shank T.M. & Von Damm K.L. 2001. Biogeography and ecological setting of Indian Ocean hydrothermal vents. *Science* 294 (5543): 818–823. https://doi.org/10.1126/science.1064574

Watanabe H. & Beedessee G. 2015. Vent fauna on the Central Indian Ridge. *In*: Ishibachi J.-I., Okino K. & Sunamura M. (eds) *Subseafloor Biosphere Linked to Hydrothermal Systems*: 205–212. Springer, Tokyo. https://doi.org/10.1007/978-4-431-54865-2_16

WoRMS Editorial Board 2020. World Register of Marine Species.
Available from http://www.marinespecies.org [accessed 1 Aug. 2020].

Zhang J., Kapli P., Pavlidis P. & Stamatakis A. 2013. A general species delimitation method with applications to phylogenetic placements. *Bioinformatics* 29 (22): 2869–2876. https://doi.org/10.1093/bioinformatics/btt499

Zhou Y., Zhang D., Zhang R., Liu Z., Tao C., Lu B., Sun D., Xu P., Lin R., Wang J. & Wang C. 2018. Characterization of vent fauna at three hydrothermal vent fields on the Southwest Indian Ridge: implications for biogeography and interannual dynamics on ultraslow-spreading ridges. *Deep Sea Research Part I: Oceanographic Research Papers* 137: 1–12. https://doi.org/10.1016/j.dsr.2018.05.001

Manuscript received: 14 December 2021
Manuscript accepted: 2 April 2022
Published on: 29 June 2022
Topic editor: Tony Robillard
Section editor: Marie-Béatrice Forel
Desk editor: Kristiaan Hoedemakers

Supp. file 1. Complementary information on the analyses of the Anatoma sample sets from the INDEX project. **Table S1** – Tabulated details of the sample set. **Fig. S1** – Graphical representation of intraspecific distances from the barcode gap analyses. **Table S2** – Intraspecific distances summary calculated using BOLD. **Fig. S2** – Graphical representation of Automated Barcode Gap Discovery (ABGD) species delimitation. **Table S3** – Tabular results of Automated Barcode Gap Discovery (ABGD) species delimitation. **Table S4** – Results of CD–Hit species delimitation. **Fig. S3** – Graphical representation of generalized mixed Yule-coalescent (GMYC) results on the basis of a Bayesian inference tree built with BEAST. **Table S5** – Generalized mixed Yule-coalescent (GMYC) results on the basis of a Bayesian inference tree built with BEAST. **Fig. S4** – Generalized mixed Yule-coalescent (GMYC) ultrametric tree with 95 individuals in BEAST including 4 references from GenBank. **Table S6** – Results of Bayesian Poisson tree processes (bPTP). **Table S7** – Analysis of Barcode Index Numbers (BINs). **Table S8** – Concordant Barcode Index Number (BIN) Report. **Table S9** – Singleton Barcode Number (BIN) Index Report.
https://doi.org/10.5852/ejt.2022.826.1841.7173